# Combustion and Emission Characteristics of Ammonia Blended Fuels in a Spark-Ignited Engine

by

Kyle Hyatali

A thesis submitted to the
School of Graduate and Postdoctoral Studies in partial
fulfillment of the requirements for the degree of

**Master of Applied Science in**
**Automotive Engineering**

Faculty of Engineering and Applied Science
University of Ontario Institute of Technology (Ontario Tech University)
Oshawa, Ontario, Canada
June 2020

# Thesis Examination Information

Submitted by: Kyle Hyatali

Master of Applied Science in Automotive Engineering

| Thesis title: Combustion and Emission Characteristics of Ammonia Blended Fuels in a Spark-Ignited Engine |
|---|

An oral defense of this thesis took place on June 26, 2020 in front of the following examining committee:

**Examining Committee:**

| | |
|---|---|
| Chair of Examining Committee | Dr. Amirkianoosh Kiani |
| Research Supervisor | Dr. Dipal Patel |
| Examining Committee Member | Dr. Martin Agelin-Chaab |
| Examining Committee Member | Dr. Xianke Lin |

The above committee determined that the thesis is acceptable in form and content and that a satisfactory knowledge of the field covered by the thesis was demonstrated by the candidate during an oral examination. A signed copy of the Certificate of Approval is available from the School of Graduate and Postdoctoral Studies.

# Abstract

Climate change and fossil fuel depletion has brought attention to the need for alternative fuels. Ammonia shows great potential as an alternative fuel because it is carbon-free and can be produced renewably. In this study the combustion and emission characteristics of ammonia blended fuels are investigated for spark ignited engines. Gasoline and heptane are explored as combustion promoters for ammonia. Experiments have been conducted on a single cylinder research engine fitted with an electronic dual fuel injection system. A parametric analysis has been conducted to investigate the effects of fuel blend ratio, engine speed, air fuel ratio, and spark timing. Blends with up to 70% ammonia have displayed good premixed combustion characteristics while reducing carbon emissions. Ammonia blends have been found to perform best at higher spark advances than baseline cases due lower flame speeds. The results show that ammonia blends are a promising alternative fuel option.

**Keywords:** ammonia; combustion; emissions; dual fuel; alternative fuel

# Author's Declaration

I hereby declare that this thesis consists of original work of which I have authored. This is a true copy of the thesis, including any required final revisions, as accepted by my examiners.

I authorize the University of Ontario Institute of Technology (Ontario Tech University) to lend this thesis to other institutions or individuals for the purpose of scholarly research. I further authorize the University of Ontario Institute of Technology (Ontario Tech University) to reproduce this thesis by photocopying or by other means, in total or in part, at the request of other institutions or individuals for the purpose of scholarly research. I understand that my thesis will be made electronically available to the public.

Kyle Hyatali
June 2020

# Statement of Contributions

Part of the work described in Chapter 4 has been presented as:

- **Hyatali, K.**, Taylor, B., and Patel, D. "Combustion and Emission Characteristics of Ammonia-Blend Fuels", The Internal Combustion Engine Division ASME International, 2020 Fall Technical Conference, Nov 1-4, 2020, Denver, USA (Accepted).
- **Hyatali, K.**, Lamothe, C., Patel, D., and Lai, J. "$NH_3$ - The Optimal Alternative Fuel", 4th Technical Poster Presentation Session, The Internal Combustion Engine Division ASME International, 2019 Fall Technical Conference, Oct 20-23, 2019, Chicago, USA.
- **Hyatali, K.**, Patel, D. and Lai, J. "Numerical Investigation of Ammonia Turbulent Flames", 4th Technical Poster Presentation Session, The Internal Combustion Engine Division ASME International, 2019 Fall Technical Conference, Oct 20-23, 2019, Chicago, USA.

In this present study, Cole Lamothe helped with the data acquisition system, and Bradley Taylor helped with experiments and processing.

# Acknowledgments

This work would not have been possible without the guidance and support of my supervisor Dr. Dipal Patel. Thank you for encouraging me and always pushing me to my full potential. I admire your work ethic and positive attitude. I am also thankful for providing me with the opportunity to present my work at an international conference.

I am appreciative of the staff at the Automotive Centre of Excellence for their technical assistance. Additionally, I would like that the Clean Energy Research Laboratory for their ammonia support.

I am especially grateful to the research assistants that helped me to complete this study and other laboratory projects. Ahmed Hussein, Allison Yuen, Billy Chan, Bradley Taylor, Cole Lamothe, Dumebi Elueme, Justin Fontanilla, Komayl Jawadi, Paul Szuflita and Paula Strach, I would like to express my gratitude for all your hard work and I wish you all the best in your future endeavors.

Most importantly I would like to thank my friends and family for their constant source of motivation and ability to always put a smile on my face. This endeavor would not have been possible without the love and support of my mother and father, Karen and Tazim Hyatali. I could not have asked for a better support system.

# Table of Contents

# List of Tables

# List of Figures

# List of Equations

# Nomenclature

### Abreviations

| | |
|---|---|
| AFR | Air Fuel Ratio |
| AKI | Anti-Knock Index |
| ALM | Accurate Lambda Monitor |
| CAD | Computer Aided Design |
| CDI | Capacitor Discharge Ignition |
| CI | Compression Ignition |
| DAQ | Data Aquisition Unit |
| DME | Dimethyl Ether |
| ECU | Engine Control Unit |
| EFI | Electronic Fuel Injection |
| EGR | Exhaust Gas Recirculation |
| HCCI | Homogeneous Charge Compression Ignition |
| HRR | Heat Release Rate |
| ICE | Internal Combustion Engine |
| LTC | Low Temperature Combustion |
| MAP | Manifold Absolute Pressure |
| MBT | Maximum Brake Torque |

| | |
|---|---|
| MIE | Minimum Ignition Energy |
| NI | National Indtruments |
| OHV | Over Head Valve |
| RON | Research Octane number |
| SCR | Selective Catalytic Reduction |
| SI | Spark Ignition |
| SSAS | Solid-State Ammonia Synthesis |
| TPS | Throttle Position Sensor |
| VE | Volumetric Efficiency |

**Species**

| | |
|---|---|
| CO | Carbon Monoxide |
| $CO_2$ | Carbon Dioxide |
| HC | Unburnt Hydrocarbons |
| NO | Nitrogen Monoxide |
| $NO_2$ | Nitrogen Dioxide |
| $NO_x$ | Oxides of Nitrogen |
| $O_2$ | Oxygen |

**Symbols**

| | | |
|---|---|---|
| $\dot{m}_f$ | Mass Flow Rate of Fuel | g/hr |
| $\dot{m}_{inj}$ | Mass Flow Rate of Fuel Injector | g/min |
| $\dot{W}$ | Indicated Power | kW |
| $\gamma$ | Specific Heat Ratio | $\sim 1.35$ |
| $\lambda$ | Lambda | |
| $\phi$ | Equivalence Ratio | |

| | | |
|---|---|---|
| $\phi$ | Equivalence Ratio | |
| $\tau$ | Indicated Torque | Nm |
| $\theta$ | Crank Angle | $^\circ$ |
| $AFR$ | Air Fuel Ratio | |
| $AFR_{stoich}$ | Stoichiometric Air Fuel Ratio | |
| $AFR_{test}$ | Tested Air Fuel Ratio | |
| $m_a$ | Mass of Air | g |
| $m_f$ | Mass of Fuel | g |
| $mep$ | Mean Effective Pressure | Pa |
| $P$ | Pressure | Pa |
| $PW$ | Injector Pulse Width | $ms$ |
| $Q_n$ | Net Heat Release | J |
| $R$ | Ideal Gas Constant | 287 $J/kg \cdot K$ |
| $S_L$ | Laminar Flame Speed | m/s |
| $SFC$ | Specific Fuel Consumption | g/kWhr |
| $T$ | Temperature | K |
| $V$ | Displacement Volume | $m^3$ |
| $W$ | Indicated Work | J |
| ST | Spark Timing | $^\circ$ $b$TDC |

# Chapter 1

# Introduction

This chapter is divided into five parts. In Section 1.1 the current problems regarding internal combustion engine fuels will be addressed. The combustion science of ammonia is reviewed in Section 1.2. In Section 1.3 the feasibility of ammonia as a fuel is explored. The thesis objectives and thesis structure is outlined in Section 1.4 and Section 1.5 respectively.

## 1.1 Current State of Art

The internal combustion engine (ICE) has dominated the automotive transportation market since the 1880's, after Nicolaus A. Otto invented the first 4-stroke engine [1]. Early model ICE's were not the most efficient, but after endless refinement to their design they incrementally improved, and are now the most efficient and cleanest to exist. However despite these improvements, the ICE remains one of the largest contributors to greenhouse gas (GHG) emissions. In the 2019 Canada's Changing Climate Report published by The Government of Canada it stated that the burning of carbon-containing fossil fuels is one of the main anthropogenic sources of $CO_2$ [2]. In the same report, multiple temperature projections were presented based on different emission reduction scenarios, a key take away from the analysis stated 'Scenarios with limited warming will only occur if Canada and the rest of the world reduce carbon emissions to near zero early in the second half of the century and reduce emissions of other greenhouse gases substantially' [2]. While plenty of advancements have been made to the ICE, they are still burning a hydrocarbon fuel that will always release carbon in the form of CO and $CO_2$ when combusted. With fossil fuels depleting and governments setting stricter emission regulations all around the world, due to the devastating effects of climate change, immediate action on finding alternative

fuel sources for our vehicles must be taken. Electric vehicles might be the choice of transport in the future, however the infrastructure to support such a drastic market change is many years away, and battery technology debatably is not yet sustainable enough to meet the demands of a green future. Action needs to be taken now, so as we wait for the electric infrastructure and technology to grow to meet our demands, one of the most promising methods to decrease GHG emissions is clean alternative fuels for full ICE powertrains or hybrid configurations. This alternative fuel approach will help to support the transition to electric transportation.

The conventional fossil fuels such as, gasoline and diesel, are apart of the planets carbon cycle, and as previously mentioned, they release harmful GHG emissions when combusted. It would be beneficial to switch away from fuels apart of the planet's natural carbon cycle, to fuels within the it's nitrogen cycle [3]. In doing so a clear choice of fuel is ammonia ($NH_3$), as it displays many properties that are sought after in an alternative fuel. First off, ammonia is carbon-free. This is extremely beneficial as carbon emissions are among the most common species that contributes to the greenhouse effect, leading to climate change [2]. Ammonia is also a high octane fuel, with a RON (research octane number) rating of $>$130 [4]. This is great for Maximum Brake Toque (MBT) timing and potential forced induction applications to improve efficiency. Moreover, clean and renewable production methods of ammonia exist [4], which would drastically reduce the well-to-wheel emissions and the carbon footprint.

## 1.2 Ammonia Combustion

While ammonia has a lot of favourable properties that makes it a great alternative fuel, there are a number of challenges associated with ammonia combustion that need to be addressed. In order to achieve good combustion properties and operating characteristics in an ICE, there are certain fuel properties that are desirable to have. Table 1.1 lists the properties for ammonia and other conventional fuels. From this table it can be seen that in comparison to the other fuels, ammonia has a high minimum ignition energy (MIE) of 8 mJ, which is the smallest amount of energy required to ignite a fuel. This makes ammonia difficult to combust, which can result in misfires and high cycle-to-cycle variation. The flammability limits range with respect to the equivalence ratio for ammonia is also narrow, which is the range of equivalence ratios that combustion can take place. Narrow flammability limits also increase the chance of misfires, and reduce operating ranges. Ammonia also exhibits a low laminar burning velocity of 7.06 cm/s, which is the speed at which a flame will propagate through a premixed fuel mixture. Low flame speeds correlate to low engine

speeds and low power outputs.

A potential solution to improve the combustibility of ammonia and increase flame speeds, is to introduce a second fuel that is easier to combust, called a combustion promoter. This fuel is injected along side the ammonia so that the two fuels can premix during intake. This results in a blended fuel that has enhanced combustion properties relative to pure ammonia. For the purposes of this research, this approach will be referred to as 'dual fuel', as it incorporate two separate fuels. This approach will be employed in this present study.

A dual fuel engine also has the benefit of increasing the heat energy content available in the cylinder. In Figure 1.1 the specific energy (heat energy per unit mass) and energy density (heat energy per unit volume) of some common fuels, including ammonia, are plotted. From this figure it can be seen that ammonia in comparison to other fuels has quite low specific energy and energy density, 18.8 MJ/kg and 1.13 $MJ/m^3$ respectively [5]. This poses a few challenges for ammonia as a standalone fuel because with a low energy density, large storage volume becomes necessary, and with a low specific energy, less heat energy is available to produce work. In terms of the storage volume, since ammonia is gaseous at standard conditions, it can easily be compressed, liquefied, and stored in a tank to reduce the overall storage volume. For instance, an ammonia tank pressurized to 10 bar increases energy density by approximately 20% [8]. Introducing a combustion promoter also decreases the ammonia fuel volume requirement. In terms of specific energy, in a dual fuel engine, the combustion promoter increases the overall specific energy by an amount dependent on the blending ratio of the two fuels.

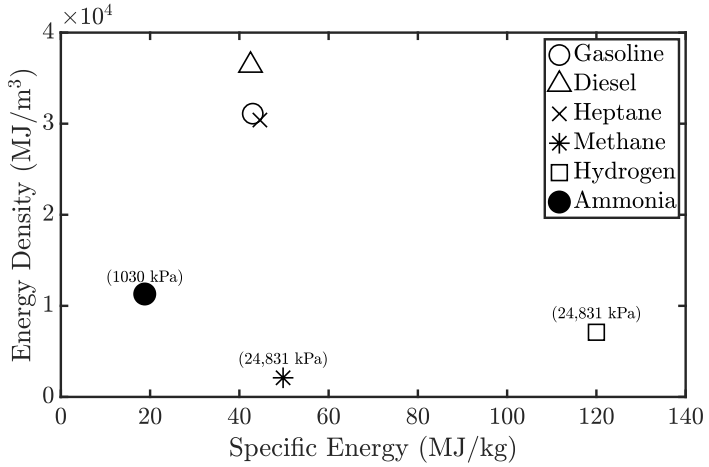


Figure 1.1: Energy comparison of fuels at standard conditions

Table 1.1: Fuel properties at standard conditions

| | Gasoline $C_nH_{1.87n}$ | Diesel $C_nH_{1.8n}$ | Heptane $C_7H_{16}$ | Methane $CH_4(g)$ | Hydrogen $H_2(g)$ | Ammonia $NH_3(g)$ |
|---|---|---|---|---|---|---|
| Molar Mass (g/mol) | $\sim$ 110 | $\sim$ 170 | 100 | 16 | 2 | 17 |
| Density (kg/m$^3$) | 698 [5] | 850 [4] | 684 [6] | 0.66 [7] | 0.08 [7] | 0.73 [7] |
| Lower Heating Value (MJ/kg) | 43.0 [1] | 42.5 [1] | 44.6 [1] | 49.8 [1] | 120.0 [1] | 18.8 [7] |
| Energy Density (GJ/m$^3$) | 34.4 [8] | 36.4 [9] | 30.4 [6] | 2.1[a] [9] | 7.1[a] [9] | 11.3[b] [9] |
| Stoichiometric AFR | 14.6 [1] | 14.5 [1] | 15.2 [1] | 17.2 [1] | 34.3 [10] | 6.1 [4] |
| Octane Rating (AKI) | 87-93 [5] | - | 0 [1] | 120 [1] | >130 (RON) [5] | 110 [5] |
| Cetane Rating | - | 40-55 [1] | 56 [11] | - | - | - |
| Auto-Ignition Temperature (°C) | 228-470 [12] | 254 [4] | 215 [13] | 630 [14] | 571 [4] | 651 [4] |
| Heat of Vaporization (kJ/kg) | 307 [1] | 270 [1] | 316 [1] | - | - | - |
| Minimum Ignition Energy (mJ) | 0.8 [15] | - | 0.24 [13] | 0.28 [7] | 0.018 [16] | 8.0 [16] |
| Flammability Limits (vol.% in air) | 1.4-7.6 [13] | 0.6-7.5 [9] | 1.2-6.7 [13] | 5-15 [13] | 4.0-75.0 [13] | 15.5-27.0 [17] |
| Flammability Limits ($\phi$) | 0.55-4.24 [4] | 0.51[c]-6.9[c] | 0.56-3.8 [19] | 0.5-1.7 [14] | 0.182-8.84 [15] | 0.724-1.46 [15] |
| Laminar Burning Velocity (m/s) | 0.43 [20] | 0.30 [20] | 0.405 [21] | 0.37 [14] | 2.91 [14] | 0.07 [22] |
| Adiabatic Flame Temperature (K) | 2266 [23] | 2350 [5] | 2274 [6] | 2223 [7] | 2383 [23] | 1850 [7] |

[a] 24,831 kPa
[b] 1,030 kPa
[c] Calculated using Eq.30 from [18]

Conventional fossil fuels are often explored as combustion promoters for ammonia since they have better combustion properties and by partially replacing the content of hydrocarbon fuels with ammonia, lowers $CO_2$ emissions are observed, when compared to pure hydrocarbon combustion [14]. Alternative fuels, like hydrogen are also considered, as hydrogen does not add carbon emission, and due to faster flame speeds of hydrogen [17] a blend of these two fuels will likely pair well to exhibit good combustion characteristics [14]. The issue with hydrogen as a fuel is that it is not easily stored and is highly unstable due to it's extremely low MIE [16]; even static can ignite a hydrogen leak, making it very dangerous [24]. The conventional fossil fuels will also enhance the combustion of ammonia, but unfortunately introduce carbon emissions. They are however safer to store and transport than hydrogen. For this reason an optimal balance of ammonia to fossil fuel would be safer, while improving combustion characteristics, and still reducing the emission characteristics of a traditional gasoline or diesel ICE.

## 1.3 Ammonia Production and Feasibility

One of the main methods of producing ammonia is through the Haber-Bosch process. This is a steam reforming process that reacts natural gas, air, and iron oxide catalysts, at high pressures and temperatures to form ammonia [7]. Air is used as a nitrogen source, while natural gas is used as both a hydrogen source and a fuel source, which means there are large amounts of carbon emissions and $NO_x$ as products of this reaction, making it an unsustainable method of ammonia production [3]. It would actually be more effective to directly power a vehicle with natural gas rather than ammonia produced from the Haber-Bosch method in terms of carbon emissions [3]. There are however clean and renewable production methods that have been developed, such as solid-state ammonia synthesis (SSAS). SSAS processes still use air as a nitrogen source, however hydrogen may come from different electrochemical processes, which obtain energy in a more environmentally friendly manor, such as solar energy or wind energy [4]. This makes SSAS processes much cleaner and even more efficient than the traditional Haber-Bosch method [4].

Since ammonia is currently widely produced through steam reforming of natural gas, the cost of ammonia is dependent on the cost of natural gas [4]. In comparison to hydrocarbon fuels like gasoline, it is substantially cheaper to produce ammonia, the average cost of gasoline is approximately \$1000/$m^3$, while only \$181/$m^3$ for ammonia [8]. The energy density for ammonia is lower than gasoline when considering ammonia stored at 10 bar and gasoline store at 1 bar, 13.6 GJ/$m^3$ and 34.4 GJ/$m^3$ respectively,

however the specific energetic cost is still much lower, \$13.3/GJ for ammonia versus \$29.1/GJ for gasoline [8].

Lastly, storage and transportation are also important criteria to consider. Ammonia is hazardous to human health and dangerous to the environment, so it must be handled with extreme care [7]. Due to the long term experience of ammonia distribution there already exists a properly functioning infrastructure system of ammonia storage and transportation that is both safe and reliable [7]. Throughout the world anhydrous ammonia is commonly transported via pipelines, railroads, barges, ships, road trailers, and even tanks and bottles [7].

Thus, with clean production methods available, a low price point determined, and storage and transportation methods established, ammonia shows feasibility and promise towards becoming a fuel for ICE's.

### 1.3.1 Proposed Ammonia System

It is well understood that ammonia engines require the use of a combustion promoter to operate effectively. This means that ammonia engines must be fitted with a dual fuel system [3]. At an initial glance it may seem difficult to implement such a system for the automotive market. Consumers may be detracted by the thought of filling two separate fuels for their vehicles. For this reason it is proposed that the ammonia system is implemented as a range extender system. For example, a traditional gasoline fueled vehicle can be fitted with a secondary ammonia fuel system as a gasoline energy replacement when needed. Such a vehicle would be able to operate on 100% gasoline if only gasoline is filled in the vehicle. The addition of ammonia becomes an option for the driver to decrease their gasoline fuel consumption. Since ammonia has a lower cost per unit volume and energetic cost [8] this system uses ammonia to reduce fuel costs, while reducing carbon emissions. The proposed system would require the development of a control strategy to determine the optimal fuel blend ratio, air fuel ratio (AFR), and spark timing for a given driving scenario. Of course further studies would need to be conducted on practical measures such at fuel consumption and costs before this system can be implemented.

## 1.4 Thesis Objectives

The aim of this thesis will be to experimentally investigate ammonia blends as fuel for spark ignited internal combustion engines. This will be accomplished by achieving the following research and design tasks:

1. Design and implement a dual fuel system for a single-cylinder research engine.
2. Investigate combustion characteristics of conventional and ammonia blended fuels.
3. Investigate emission characteristics of conventional and ammonia blended fuels.

## 1.5 Thesis Structure

This thesis consists of five chapters that outline the research work completed and its findings. Chapter 1: Introduction, has discussed some of the key details regarding ammonia combustion and its feasibility as a fuel, and has also outlined the objectives of this thesis. In Chapter 2: Literature Background, an overview of the current research landscape regarding ammonia combustion is reviewed, including where there are observed gaps in the literature and the novelties of this research. Chapter 3: Experimental Setup, the design specifications of the experimental unit is covered in detail.

Chapter 4: Results and Discussion is divided into three sections, Parametric Analysis Outline, Combustion Characteristics, and Emission Characteristics. The Parametric Analysis Outline portion discusses the tests completed in this present study. In the Combustion Characteristics and Emission Characteristics sections, the effects of engine speed, lambda, spark advance angle, and hydrocarbon to ammonia fuel blend ratios are explored. In-cylinder pressure traces, heat release rate (HRR) traces, and performance measurements are used to gain an understanding of the nature of the combustion process in the Combustion Characteristics section. The Emission Characteristics section analyzes the variations in five main exhaust species, being carbon dioxide ($CO_2$), carbon monoxide (CO), oxygen ($O_2$), unburnt hydrocarbons (HC), and nitrogen dioxide ($NO_2$).

Finally, Chapter 5: Conclusions summarizes the key findings of this work, its significance, and outlines the next steps that should be taken to continue and improve upon this research.

# Chapter 2

# Literature Background

In this chapter the research background of ammonia fuel in ICE's will be explored. The chapter is divided into four sections. Section 2.1 provides a brief look into the history of ammonia in ICE's. Section 2.2 discusses the current research and findings regarding ammonia fuel properties. Section 2.3 discusses the dual fuel approach, combustion promoters, compression ignition (CI) and spark ignition (SI) applications, and selective catalytic reduction. Finally the observed gaps in the literature are examined in Section 2.4.

## 2.1 History of Ammonia Fuel

The use of ammonia as a fuel source dates back many years. In 1822 Sir Goldsworthy Gurney proposed an engine he developed to drive a small locomotive using ammonia [7]. Although, it wasn't until 1905 that Ammonia Casale Ltd. developed the first small scale motor [7]. Ammonia has also been used as a hydrogen source for a vehicle by Norsk Hydro, which used on-board reforming of ammonia to produce hydrogen [7]. One of the greatest achievements to date was in 1942 during World War II when Belgium used ammonia fuel in their buses [7]. Due to a shortage of diesel at the time, alternative fuel sources needed to be employed [3]. A coal gas and ammonia blend was used, where the coal gas was used as a combustion promoter for the ammonia [3]. Moving forward, research in the refinement of ammonia engines for military applications took place [3]. Pure ammonia engines were unsuccessful, so a number of methods to improve ignition were explored including, an increase spark energy, compression ratio, using forced induction, and combustion promoters [7]. Little development took place after the 1970's, but the field gained momentum in the 1990's onward [7]. Today, the combustion of ammonia and it's applications is a

widely studied and growing research topic globally.

## 2.2 Ammonia Fuel Properties

Combustion characteristics are dependent on fuel properties, which are typically determined in controlled combustion chambers or combustors. Such experiments are essential to engine design. In order to effectively use ammonia as a fuel in IC applications, these properties must be well understood. MIE for instance plays a critical role in the requirement of (SI) engine ignition systems. An early study found that a MIE of 8 mJ was need to ignited a premixed ammonia/air mixture, which was higher than hydrocarbon/air mixtures, concluding that increased ignition-system-energy capacity would be necessary to use ammonia in a system designed for hydrocarbon fuels [15]. Additionally, laminar flame speeds ($S_L$) are important as they dictate engine speeds and power outputs in both SI and CI engines. Y. Li *et al.* studied the effects of equivalence ratio ($\phi$) on $S_L$ of premixed ammonia/air mixtures in a spherical combustion chamber. The study found that with respect to $\phi$, $S_L$ increased to a point and then decreased, peaking at 7.06 cm/s in slightly rich conditions of $\phi = 1.1$ [22]. These trends can be seen in Figure 2.1, which compares the experimental work to computed reaction mechanisms. The reaction mechanisms used were, GRI 3.0, Tian, and Konnev. Each mechanism has limitations, responsible for variance to the experimental work. The laminar flame speeds found numerically and experimentally are significantly lower than a hydrocarbon fuel [22], providing support for the need of combustion promoters.

Ignition delay is a important parameter specific to CI engines, as it indicates the time delay between the start of injection and the start of combustion. The ignition delay time for ammonia was studied by M. Pochet *et al.* in a rapid compression machine [25]. It was noted that increased pressure resulted in shorter ignition delay times, highlighting the benefits of high compression engines, or forced induction applications.

A benefit of ammonia being composed of only nitrogen and hydrogen is that it does not emit carbon or soot emissions during combustion. However, there is still $NO_x$ emissions, which are toxic and harmful to the environment [7]. Studies in emission characteristics are crucial as they help determine methods of controlling harmful pollutants. $NO_x$ emissions are primarily formed due to high temperatures [14], which cause nitrogen and oxygen to react with another; this is thermal $NO_x$ emissions. $NO_x$ emissions are also formed due to reactions with the bonded nitrogen in ammonia [5],

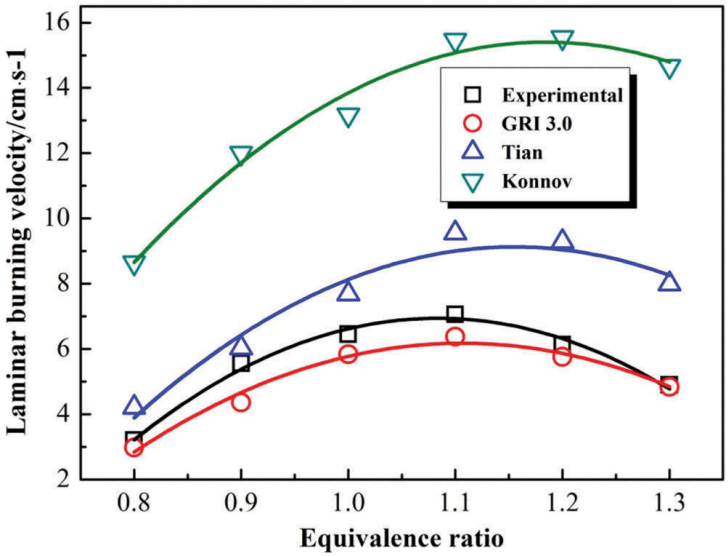


Figure 2.1: Ammonia/air laminar flame speed at various equivalence ratios (Figure from [22])

called fuel $NO_x$. Generally, the high octane value and the low flame temperature of ammonia produces lower thermal $NO_x$ emissions, making it suitable for high compression engines [26]. Shock tube experiments and kinetic modeling by B. Shu *et al.* determined that as ammonia/air mixture get richer ($\phi$ increases), $NO_x$ significantly decreases [27]. At low temperatures and highly fuel-rich conditions, $NO_x$ emission are extremely low [27]. A. Hayakawa *et al.* saw similar trends in experiments using a swirl combustor [28].

## 2.3 Dual Fuel Ammonia Engines

Since pure ammonia ICE's are not feasible [7], and pure ammonia combustion has proven to exhibit poor characteristics, combustion promoters in dual fuel applications are used to the improve combustion characteristics. Dual fuel methods are the only reasonable method of effectively combusting ammonia in ICE's [3]. A number of different fuels are commonly explored as combustion promoters, which can be used in either CI and SI applications. These topics will be examined in this section, as well as the selective catalytic reduction (SCR) exhaust after-treatment system.

### 2.3.1 Combustion Promoters

Fuels with higher flame speeds and heat release rate (HRR), such as conventional hydrocarbon fuels, are commonly explored as combustion promoters [14]. A review on the science of ammonia combustion by H. Kobayashi *et al.* states that ammonia

blended hydrocarbon fuels are important as a step towards a carbon free society [14]. J. Li *et al.* has also indicated that alternative fuels like hydrogen could be used to enhance the low flame speed of ammonia [17]. Modeling by A. Yapicioglu and I. Dincer shows that combustion promoters in general can enhance combustion characteristics of ammonia, while maintaining good emission characteristics [29]. Some results from this modeling analysis are shown in Figures 2.2 and 2.3, which show $CO_2$ and $NO_x$ trends against ammonia to combustion promoter ratio [29]. It can be seen in both figures that as ammonia concentration is increased, the emissions decrease, which is true for all the fuels plotted. Sections 2.3.1.1 to 2.3.1.5 reviews some specific combustion promoters.

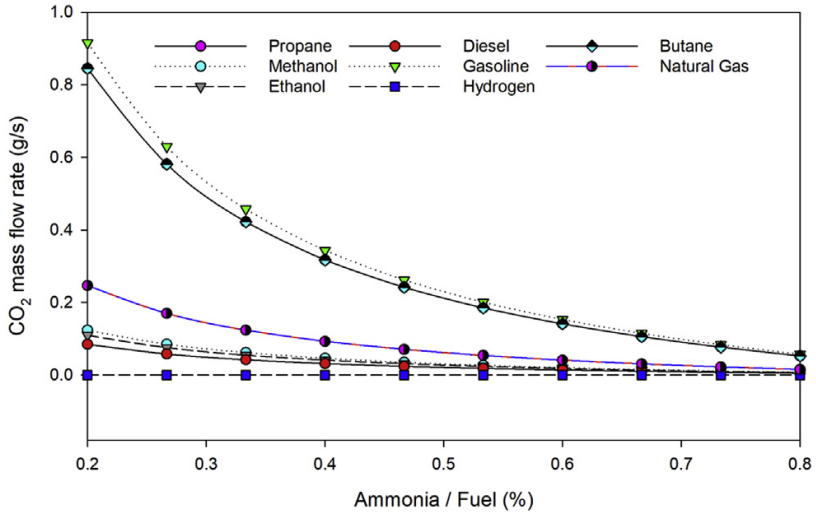


Figure 2.2: $CO_2$ emissions of different ammonia fuel blends (Figure from [29])

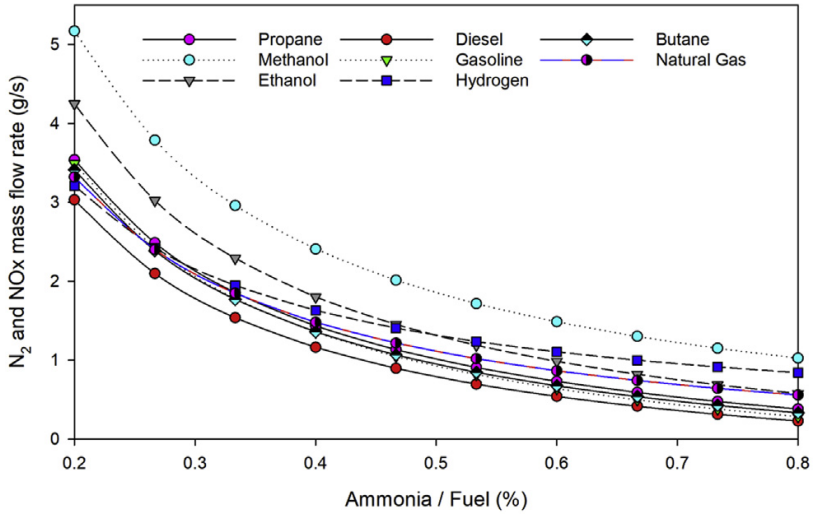


Figure 2.3: $NO_x$ emissions of different ammonia fuel blends (Figure from [29])

#### 2.3.1.1 Gasoline

Gasoline is frequently researched as a combustion promoter for ammonia engines because it is a common IC fuel with relatively high flame speed and low MIE, presented in Table 1.1. Gasoline/ammonia mixtures are mainly studied in SI engines, which is covered in Section 2.3.3.

#### 2.3.1.2 Diesel

Diesel/ammonia mixtures are often studied in CI engines [9]. Due to the high autoignition temperature of ammonia, diesel, which has a much lower autoignition temperature, is used to ignite the ammonia (see Table 1.1). Since ammonia has a high ignition energy and octane rating, it can withstand the higher compression ratios without knocking. Diesel/ammonia mixtures are discussed further in Section 2.3.2.

#### 2.3.1.3 Heptane

It can be seen from Table 1.1 that heptane exhibits some desirable properties of a combustion promoter such as a relatively high flame speed in comparison to ammonia, and a low MIE. However, little research involving heptane as a combustion promoter for ammonia exists. Heptane and ammonia combustion was modeled for CI motors by Zhong *et al.* who found that as heptane concentration increased, ignition temperature required decreased [7]. Also, in a recent study L. Yu *et al.* numerically modeled and experimentally tested the low-temperature autoignition of heptane/ammonia mixtures in a rapid compression machine [30]. The study found that increased heptane, decreases ignition delay times [30]. No research was found on heptane/ammonia mixtures in SI applications.

#### 2.3.1.4 Methane

Methane/ammonia mixtures have been extensively researched in many studies. As seen from Table 1.1, methane demonstrates favourable properties sought after in a combustion promoter, such as high flame speed, high specific energy, and low MIE. Methane is also gaseous and similar in density as ammonia, aiding in premixing [7]. Experimental tests in a combustion chamber and simulation studies by both E. C. Okafor *et al.* have shown that as ammonia is added to methane/air combustion, laminar flame speeds decrease [31], which is to be expected based on the low flame speed of ammonia. P. F. Henshaw *et al.* saw similar results in simulations and experimentally with a flat flame burner [32]. The study also noted an increase in NO emissions with ammonia addition, with minimal effect on CO formation [32]. A significant re-

duction in $CO_2$ emissions was observed by J. W. Ku *et al.* in numerical studies and experimental studies with a counterflow burner, however the study stated further investigation is required to reduced enhanced $NO_x$ emissions [33]. To reduce $NO_x$ emissions and increase flame stability, A. Valera-Medina *et al.* noted that stratified injection strategies, opposed to premixed, should be used with methane/ammonia mixtures, from numerical and experimental studies with a swirl burner [34]. Stratified injection strategies refer to direct injection (DI) in terms of ICE's, which can be used in both SI and CI engines.

#### 2.3.1.5 Hydrogen

Hydrogen is a popular combustion promoter researched for ammonia in SI and CI engines. It is an attractive combustion promoter because it is carbon-free, so it does not add any direct carbon emissions. Also, it has very high flame speeds, high specific energy, and low MIE (see Table 1.1). Additionally, in a hydrogen/ammonia vehicle, the hydrogen can be produced onboard from ammonia electrochemically [35], meaning the consumer would only need to fill a single fuel. Experimental analysis by J.Li *et al.* in a combustion chamber indicated that the addition of hydrogen to an ammonia/air mixture increases the flame speed to a favourable level [17]. Laminar flame speeds have shown to exponentially increase with increased hydrogen by H. Kobayashi *et al.* [14]. Ammonia was also shown to decrease the combustion temperatures of hydrogen/air mixtures, which lowers the thermal $NO_x$ emissions [17]. A numerical study by J.Li *et al.* observed an enhancement in the HRR of a premixed laminar ammonia flames with added hydrogen, as well as a reduction in $NO_x$ emissions under fuel rich conditions [36]. The ignition delay of ammonia and ammonia/hydrogen mixtures under low temperature combustion (LTC) conditions were numerically and experimentally studied with a rapid compression machine by M. Pochet *et al.* [25]. LTC methods are employed to reduce the production of thermal $NO_x$. In the study hydrogen was shown to produce a significant decrease in ignition delay when the ammonia/hydrogen mixtures were greater than 10% hydrogen in volume [25]. In order to meet these hydrogen demands, a large hydrogen reserve or onboard reforming would be necessary [25]. The study also noted that ammonia/hydrogen mixtures are suitable for high compression ratio engines, or engines with forced induction [25].

### 2.3.2 CI Applications

CI engines use high compression ratios to reach the autoignition temperature of their fuel source. High compression ratios increase combustion temperatures and ther-

mal $NO_x$ formation [9]. To lower combustion temperatures and $NO_x$ levels, ammonia blends are used [37], due to the lower adiabatic flame temperature of ammonia (shown in Table 1.1). In ammonia blends, the ammonia also replaces part of the carbon fuel, reducing carbon emissions [37]. Ammonia is however highly resistant to autoignition, requiring incredibly high compression ratios of 35:1 to 100:1 to operate in pure ammonia engines [9]. Poor combustion and operating characteristics are observed due to a high autoignition temperature, low flame speed, and narrow flammability limits [9]. For this reason ammonia combustion in CI engines requires a secondary fuel, similar to a combustion promoter, to work as a pilot and ignite ammonia/air mixtures [9]. These secondary fuels must have a low autoignition temperature to trigger combustion, and high cetane values for optimal performance, to reduce ignition delay times, and increase combustion efficiencies. [9].

Diesel has been commonly researched in dual fuel ammonia engines, and have shown to operate as low as 15.2:1 compression ratio [9]. A. Reiter *et al.* used diesel/ammonia mixtures in a 2008 chemical kinetic study and experimentally analysis with a dual fuel CI engine [37]. The engine used gaseous ammonia port injection and diesel direct injection as a pilot fuel [37]. Results showed that similar engine torque can be achieved with different diesel/ammonia ratios, and ammonia energy replacement can be as high as 95% [37]. $CO_2$ emissions reduced in a near proportional manner to ammonia energy ratio and $NO_x$ reduction was observed for ammonia ratios below 60% [37]. The reduction in $NO_x$ was due to the lower combustion temperatures of ammonia, which had the adverse effects of increasing HC emissions [37]. Low combustion efficiencies of ammonia are seen due to low flame speed and long quenching distance, leading to trapped fuel in crevice volumes [9]. Simulations by J. Lasocki *et al.* in diesel/ammonia dual fuel CI engines also saw decreases in carbon emissions, but increased $NO_x$ emissions under heavy loads [38]. In 2011 authors A. Reiter *et al.* continued experimental work with diesel/ammonia mixtures in a 17:1 compression ratio dual fuel CI engines [5]. Similar emission trends were found as previous, also noting that soot emissions decreased with increased ammonia concentration [5]. Pressure and HHR traces showed increasing ammonia concentration to decrease peak pressures and increase ignition delay times [5]. Combustion efficiency was relatively high, but ammonia exhaust concentration was still above regulation [5]. The study mentioned that in order to bring diesel/ammonia mixtures to market, different injection strategies would need to be tested and/or exhaust after treatment options would need to be developed [5].

Other fuels have also been tested with ammonia in CI engines including hydrogen

[39], bio-diesel [37], and dimethyl ether (DME) [40]. Ammonia/hydrogen blends were used in conjunction with homogeneous charge compression ignition (HCCI) LTC method by M. Pochet *et al.* in an experimental and simulation study [39]. The engine performed with up to 70% ammonia content by volume, with HCCI combustion achieved through intake pressures of 1.5 bar and heating of 475K, however higher compression ratios could reduce these values [39]. Cylinder temperatures above 1300K were necessary to see combustion efficiencies similar to hydrogen, given the high ignition delay due to ammonia [39]. High $NO_x$ levels were detected as a result of the fuel bound nitrogen, and not thermal $NO_x$, as cylinder temperatures remained around 1400K, which is below the 1800K thermal $NO_x$ limit [39]. The study concluded that fuel $NO_x$ emissions could be cancelled with exhaust gas recirculation (EGR) [39]. DME was used by C. W. Gross in a CI engine, and was shown to further reduce carbon emissions in comparison to diesel or bio-diesel mixtures [40]. In this study, DME/mixtures were premixed prior to injection, and were direct injected [40]. Results showed ammonia content to increase ignition delay times, and limit engine load due to lower flame speeds and high autoignition temperatures [40]. A decrease in combustion temperatures was observed, which increased HC and CO emissions [40]. $NO_x$ emissions increased due to the nitrogen in the ammonia [40].

### 2.3.3 SI Applications

SI applications are widely studied for ammonia mixtures, with vast literature showing them to be viable options for the challenging fuel. Ammonia is well suited for SI engines as it can take high compression ratios without the risk of knock, due to the high octane rating [41]. The high octane rating also allows knock free maximum brake torque (MBT) timing, where other fuels like gasoline are knock limited [42]. Also, SI engines produce lower thermal $NO_x$ than CI engines due to the lower combustion temperatures [9]. Thus ammonia can replace carbon fuel content, while achieving low $NO_x$ emissions. A pure ammonia SI engine was attempted with a very high 30:1 compression ratio, but was unsuccessful [7]. As discussed in detail, combustion promoters are a necessity for ammonia combustion in ICE's. Due to the low flame speed, and high MIE of ammonia, fuels with higher flame speeds and lower MIE are used to promote the combustion of ammonia in SI engines.

Gasoline is a commonly used combustion promoter for ammonia in SI engines because it is widely used in the automotive market, and has high flame speeds and lower MIE in comparison to ammonia. In a 2008 study by S. Grannell, stoichiometric gasoline/ammonia mixtures were used in an SI engine [42]. This study found that

a significant fraction of gasoline could be replaced by ammonia, 70% ammonia and 30% gasoline at wide open throttle, with higher ammonia concentrations when supercharged [42]. It was also found that while gasoline only was unable to reach MBT timing due to knock, gasoline/ammonia mixtures were able to achieve MBT timing without knock [42]. Higher thermal efficiency and BMEP (brake mean effective pressure) was also observed for gasoline/ammonia mixtures [42]. A compression ratio of 10:1 was recommended as higher compression ratios have diminishing returns on thermal efficiency and reduce the margin between MBT timing and knock [42]. Ammonia has also been premixed with gasoline prior to injection in work by Haputhanthri *et al.*, which used a high pressure cell to create a single liquid fuel comprised of gasoline and ammonia [43]. A number of blends where made and tested, including an E30 gasoline blend (gasoline with 30% ethanol) with 17.35% liquid ammonia by volume [43]. Results showed that engine performance remained mainly unaltered, with increased torque and power at high loads [43]. Engine performance improvements were also seen in a study using an SI engine with gasoline port injection and gaseous ammonia direct injection by K. Ryu *et al.* [44]. In the study, injection strategies were developed and gasoline/ammonia mixtures were shown to increase engine power compared to pure gasoline, with advanced injection timing and injection duration [44]. Peak cylinder pressures and combustion temperatures decreased slightly, as expected due to the lower flame temperature of ammonia, while brake specific energy consumption remained comparable to gasoline alone [44]. $NO_x$ emissions significantly increased due to the formation of fuel $NO_x$ and ammonia slip, while CO emissions slightly decreased and HC emissions increased due to lower combustion temperatures [44].

Hydrogen is another popular combustion promoter of ammonia in SI engines because it is carbon free and has superior combustion characteristics to ammonia. For instance, up to 20% hydrogen volume was used with ammonia to reduce misfires and cycle variations, while providing good indicated efficiencies and work output, in a study by C. Lhuillier *et al.* [41]. S. Frigo *et al.* used between 7% and 11% hydrogen to ammonia energy ratio depending on load in an SI engine that used on-board catalytic reforming to produce hydrogen [45]. A decline in power compared to pure gasoline was observed, but with low $NO_x$ emissions [45]. C.S. Mørch *et al.* tested various excess air ratios, compression ratios, and ammonia to hydrogen blend ratios in a 2010 study using an SI engine [16]. In the study, a 10% volume of hydrogen performed the best, with increased efficiency and power [16]. Highest $NO_x$ emissions were observed when hydrogen content was high and excess air ratios were between 1.1 and 1.4, due to increased combustion temperatures [16].

### 2.3.4 Selective Catalytic Reduction

A selective catalytic reduction (SCR) system uses ammonia injection in the exhaust to reduce nitrogen oxide emissions. Only small amounts of ammonia are used to react with the nitrogen oxides in the exhaust to form nitrogen and water [16]. Simulations studies saw that nitrogen emissions in the exhaust could be completely eliminated using the SCR [46]. In dual fuel ammonia engines, a SCR system is easy to implement since ammonia is already stored onboard. It should be noted that exhaust after-treatment devices such as the SCR can be used in SI and CI engines, independent of any additional fuels.

## 2.4 Thesis Novelty and Research

From literature it can be seen that ammonia can be used to lower both carbon and $NO_x$ under certain conditions. Although both CI and SI engines did experience elevated HC, CO, and $NO_x$ emissions typically. To reduce these emissions, further research must be carried out to develop and refine reduction strategies. Exhaust after-treatment options should also be considered such as reformulated ammonia engine specific catalytic converters [42] and SCR [16]. Nevertheless, CI and SI engines both operated effectively using dual fuel ammonia systems, with improved performance in some cases, supporting continued development of ammonia fueled engine.

In this present study a 4-stroke single cylinder dual fuel SI engine has been utilized. The novelty of this research is that ammonia and heptane have been experimentally analyzed in an SI dual fuel engine for the first time. Other than autoignition studies by L. Yu *et al.* and CI simulations by Zhong *et al.*, there has not been any significant research on heptane/ammonia mixtures, and to date, no research regarding heptane/ammonia mixtures in SI engines has been found. In comparison to a common combustion promoter like gasoline, which has a high specific energy, low MIE, and fast burning velocity, heptane also exhibits high specific energy and a fast burning velocity, but with a lower MIE energy and octane rating of 0 (see Table 1.1). For these reasons, heptane is very easy to ignite, making it a potentially better combustion promoter than gasoline in SI applications.

Testing in this thesis will investigate and compare the combustion and emission characteristics of four fuel groups.

1. gasoline only (baseline)

2. gasoline/ammonia blends

3. heptane only (baseline)

4. heptane/ammonia blends

Control variables will be engine speed, lambda, spark timing, and ammonia to hydrocarbon blend ratio. In-cylinder pressure traces, HRR traces, and performance measurements will be used to analyze the combustion characteristics, and $CO_2$, CO, $O_2$, HC, and $NO_2$ exhaust species will be measured for emissions analysis.

# Chapter 3

# Experimental Setup

In this chapter the experimental setup used to conduct this research is discussed in detail. The chapter is divided into three sections. In Section 3.1 the design specifications for each component of the experimental unit are discussed. Section 3.2 summarizes design of the experimental unit. Lastly, Section 3.3 reviews the limitations of the experimental unit.

## 3.1 Design Specifications

In this section the components necessary to construct the experimental setup are discussed in detail. These components include the engine, the fuels and their specific delivery methods, the engine control unit (ECU), the data acquisition unit (DAQ), and the engine stand.

### 3.1.1 Engine

The engine chosen for this study was a single cylinder naturally aspirated 4-stroke SI engine. This configuration was chosen because 4-stroke SI engines have shown promise with ammonia blended fuels (see Section 2.3.3). The engine has a displacement volume of 0.208L, a compression ratio of 8.5:1, and uses an overhead valve arrangement. The engine was originally gasoline powered and carbureted, however it was converted to a dual fuel engine to allow for the use of combustion promoters, and converted to electronic fuel injection (EFI) to provide better control over fuel and ignition. Details on the dual fuel system are provided in Section 3.1.2, and the EFI system is discussed in in Section 3.1.3. Engine modifications include, the dual fuel system, EFI conversion, and additional sensors for the DAQ system. No modifications of engine internals took place. No exhaust after-treatment devices were used.

### 3.1.2 Fuel Delivery

In this study ammonia fuel is blended with a combustion promoter via a dual fuel system. Both fuels are injected separately into the intake stream through their own fuel systems, and blend within the inlet runner and cylinder. The fuels used as combustion promoters will be either gasoline or heptane.

In a typical gasoline powered vehicle, fuel is delivered to the cylinder by a port injection method. Liquid gasoline is stored in a tank at atmospheric conditions and an electric fuel pump is used to pressurize and transfer the fuel through metal and rubber lines to an electromechanical fuel injector. The injector sprays and atomizes the gasoline into the intake stream, where it mixes with the air and becomes combustible. A similar liquid port injection system was developed for this experimental unit which can be used for a variety of fuels, including gasoline and heptane. The fuel system is equipped with an adjustable fuel pressure regulator set to 3 bar, as this is the operating pressure of the fuel injector.

For the ammonia fuel system a port injection method was also employed, however with a few variations to the previous system. To begin, liquefied anhydrous ammonia was stored in a tank with a gauge pressure of 7.86 bar. From the tank the out flow of ammonia was regulated to a pressure of 3 bar, which turns ammonia into a gas. For this reason a gaseous electromechanical fuel injector was used, opposed to the traditional liquid type. A gaseous injection system was used instead of a liquid system, because liquid ammonia has a high heat of vaporization [4], which improves volumetric efficiency, but also significantly cools the intake charge. This can be beneficial for SI engines with high compression ratios or forced induction in order to reduce the chance of knock, however lower intake temperatures are not required for this experimental unit, due to the lower compression ratio.

Both fuel injectors were attached to the engines throttle body, shown in Figure 3.1. The hole for the liquid injector is clearly shown in 3.1a directly on top of the throttle body. In this same image, on the left hand side a servo motor was installed (not shown here) to actuate the throttle, and on the right hand side the throttle position sensor (TPS) can be seen. In Figure 3.1a a thin nipple can be seen on the right side of the throttle body. This nipple was removed, and a threaded hole was drilled and tapped for the ammonia injector to directly thread into.

Lastly, in order to connect the throttle body to the engine, a custom intake adapter needed to be designed and manufactured. Figure 3.2 shows a 360° CAD model of the adapter designed and 3D printed for this purposed. The component was printed using

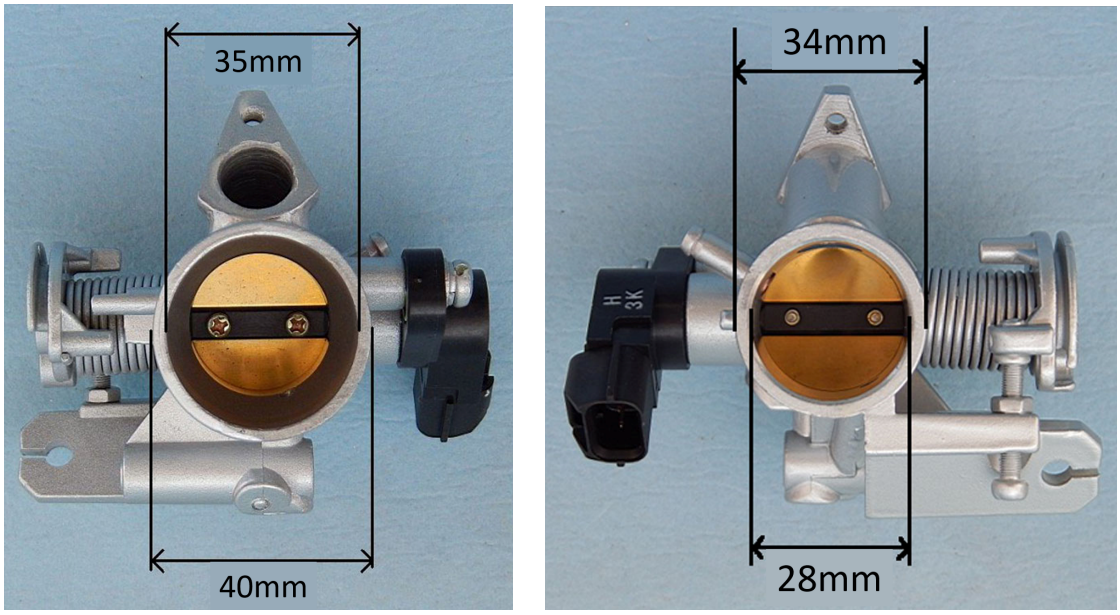


(a) Ambient side (b) Engine side

Figure 3.1: Throttle body

a nylon filament, as nylon is safe to use with gasoline, heptane, and ammonia. The adapter measures only 46mm in length, as it was important to keep this component short to minimize the distance of the injectors from the cylinder. The nipple shown in Figure 3.2c is for the manifold absolute pressure (MAP) sensor and the hole shown in Figure 3.2f is for intake air temperature sensor.

### 3.1.3 Engine Control Unit

It was crucial that the fuel and ignition were completely controlled. For this reason, a fully programmable standalone ECU was required. The ECU along with all the required sensors and components were sourced from a company called Ecotrons. This included, the ECU, the wiring harness, a throttle body, a capacitor discharge ignition (CDI) system, both liquid and gaseous fuel injectors, a hall-effect sensor (engine speed), a MAP sensor, intake air and engine block temperature sensors, and an oxygen sensor. The ECU is programmed using the Ecotrons tuning software EcoCAL, which operates on the speed density principal.

The speed density principal uses the ideal gas law to calculate the mass of air ($m_a$) through the engine per cycle (Eq. 3.1), and the required mass of fuel ($m_f$) necessary to achieve the desired air fuel ratio (AFR).

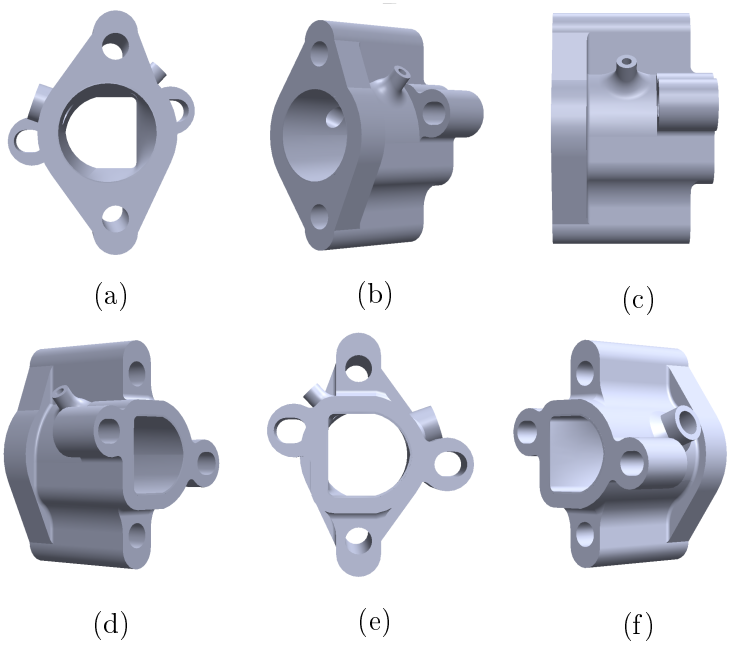

Figure 3.2: Custom intake adapter CAD model

$$\begin{aligned} PV &= mRT \\ m_a &= \frac{PV}{RT} \end{aligned} \tag{3.1}$$

The pressure term ($P$) comes from the MAP sensor, the temperature term ($T$) comes from the intake air temperature sensor, and the ideal gas constant ($R$) is specific to air. The volume term ($V$) is the displacement volume, assuming 100% volumetric efficiency (VE). However, since VE changes depending on engine speed and load, VE is a tunable parameter in the ECU to control the mass of fuel. The oxygen sensor is a tuning tool used to determine the AFR and calibrate the volumetric efficiency for a given load and engine speed. Once $m_a$ [g] is determined, the necessary $m_f$ [g] is calculated based on the desired AFR, seen in Eq. 3.2.

$$\begin{aligned} AFR &= \frac{m_a}{m_f} \\ m_f &= \frac{m_a}{AFR} \end{aligned} \tag{3.2}$$

Finally, once the desired $m_f$ is known, the necessary injector pulse width (PW)

[ms] is calculated based on the rated mass flow rate of the fuel injector ($\dot{m}_{inj}$) [g/min], seen in Eq. 3.3.

$$\begin{aligned} m_f &= \frac{PW}{60000} \times \dot{m}_{inj} \\ PW &= \frac{m_f}{\dot{m}_{inj}} \times 60000 \end{aligned} \tag{3.3}$$

The ignition timing is also tuned in the EcoCAL software, this however is a direct process unlike the fuel. EcoCAL can also display live sensor measurements, injector pulse widths, spark timing, as well as data log all channels to a computer connection. Data logging is useful for tuning and post-processing analysis.

### 3.1.4 Data Acquisition Unit

In order to study combustion and emissions characteristics from the engine, additional instruments were needed. For combustion analysis an in-cylinder pressure transducer and optical encoder were used to map in-cylinder pressure, heat release rate (HRR), and obtain performance measurements. To study emissions characteristics, a five gas analyzer was used to record carbon dioxide ($CO_2$), carbon monoxide (CO), oxygen ($O_2$), unburnt hydrocarbons (HC), and nitrogen dioxide ($NO_2$) exhaust species. Additional sensors were installed to monitor the liquid fuel pressure and exhaust temperature. All data streams were synced and recorded using a National Instruments (NI) data acquisition system, which was programmed using LabVIEW 2019. Microsoft Excel and MATLAB were used for post-processing analysis.

Figure 3.3 shows a schematic of the engine and all of its sensors and outputs. In this figure the red lines refer to sensors and output connected to the ECU, while blue lines refer to sensors connected to the DAQ.

In Figure 3.4, a summary of the data collection is provided. In this figure the individual electronic components that control and monitor the engine are divided into blocks. The lower blue block shows the engine related components, and the upper red block shows the additional external measurement components used with the DAQ. The arrows indicate the direction of communication. All of the listed parameters can be monitored and used for post-processing analysis.

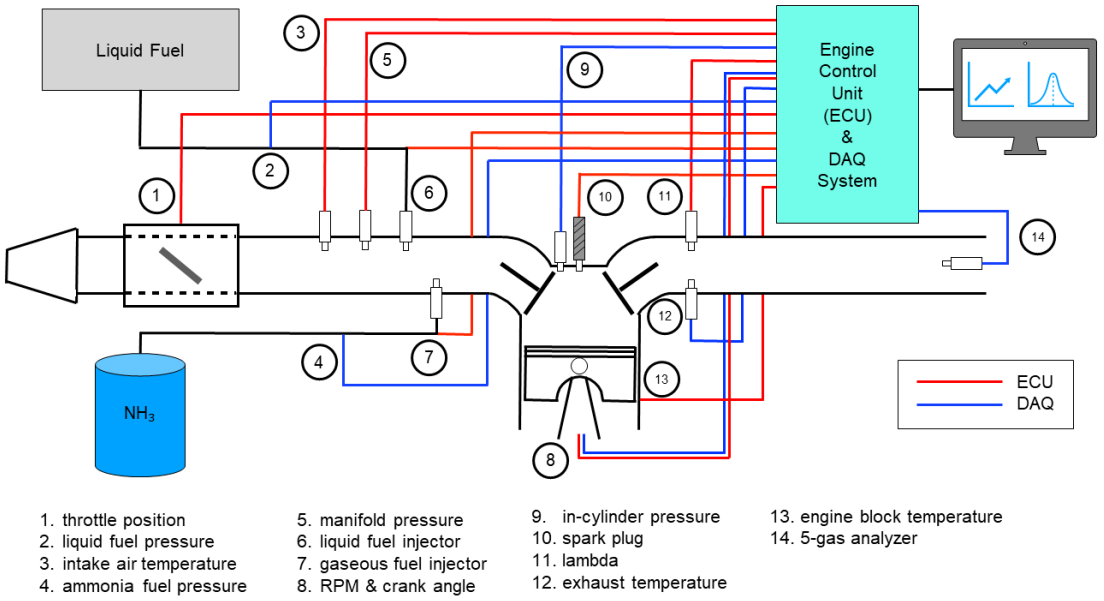


Figure 3.3: Engine schematic

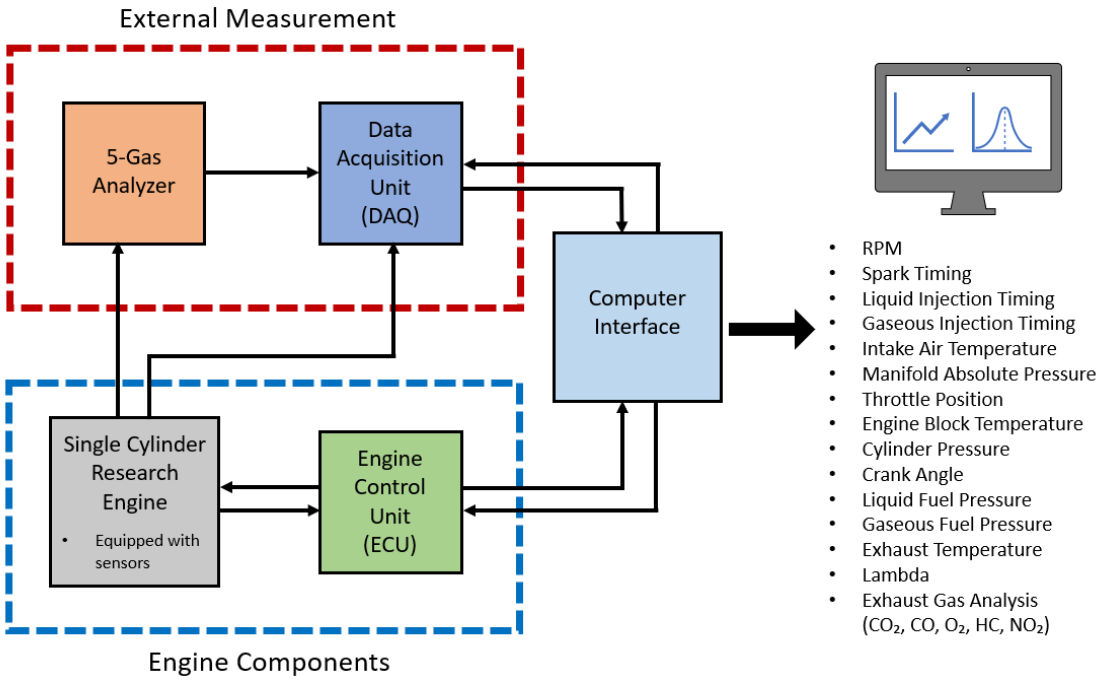


Figure 3.4: Block diagram overview of data collection

#### 3.1.4.1 In-Cylinder Pressure Measurement

The in-cylinder pressure transducer used in this research was a Kistler 6013CA. The sensor reads cylinder pressure and outputs a corresponding charge value in units of

picocoulomb (pC). The NI DAQ however uses an analog voltage module that requires a voltage from -10 to 10V. To convert the pC current from the sensor to an analog voltage, a Kistler 5073 charge amplifier is used. The sensor outputs a current to the charge amplifier, and from the charge amplifier an analog voltage is sent to the NI DAQ, which is calibrated to a corresponding pressure value. A 720 pulse per revolution (ppr) BEI sensors H25 optical encoder was used to measure the engine crank angle.

To obtain the in-cylinder pressure measurement the transducer needed to be installed into threaded hole in the cylinder head of the engine. To do this, the cylinder head was uninstalled from the engine and a hole was carefully drilled and tapped. In Figure 3.5 an image of cylinder head can be seen, which shows the sensor installed. In this figure, the threaded hole on the bottom right is for the spark plug and the hole on the bottom left is where the pressure sensor is installed.

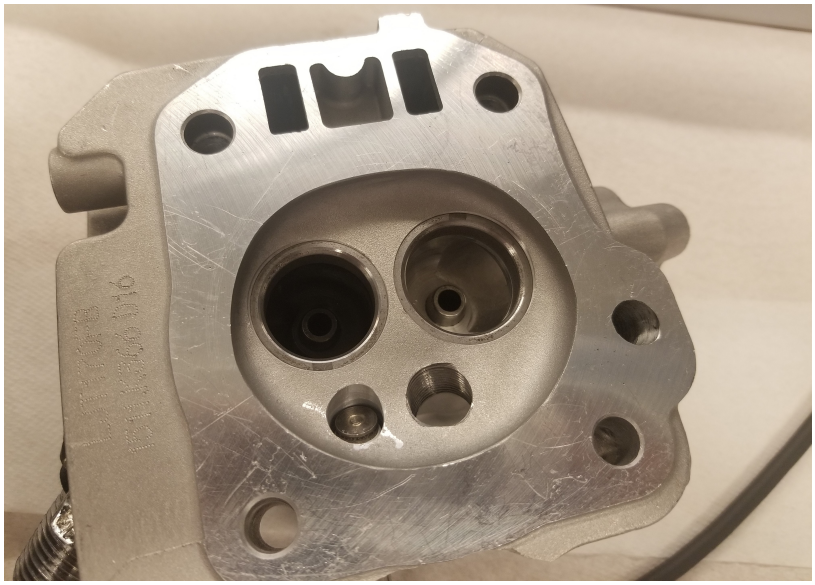

Figure 3.5: In-cylinder pressure transducer installed in cylinder head

#### 3.1.4.2 Emissions Measurement

For the emissions analysis a five gas analyzer from EMS Gas was utilized, model 5003. The gas analyzer is capable of measuring $CO_2$, CO, $O_2$, HC, and $NO_2$ exhaust species via a probe that goes into the exhaust pipe of the engine. $CO_2$, CO, and $O_2$ are measured in units [%] and HC and $NO_2$ are measured in units [ppm]. All species are measured with respect to volume. Lambda and AFR readings are also available, however these are only accurate if the correct fuel is selected on the unit out of the limited options. Custom fuels cannot be input, so lambda and AFR on this unit are

only accurate when testing 100% gasoline for this research. $NH_3$ measurements in the exhaust are not available, making $NH_3$ slip an unknown factor and limitation of the setup. The unit displays live species readings on the screen at a sample rate of 1.5 seconds per 25 ft. of hose length used. Since the unit uses a 25 ft. hose, this equates to a 0.67 Hz sample rate. The analyzer was configured to record data to the NI DAQ for further processing.

### 3.1.5 Engine Stand

To operate the engine and house all of the additional components, a custom engine stand was designed and manufactured. The main requirements of the engine stand were that the engine could be fully operated and controlled from the stand, all components had a secure location, the stand was isolated from vibration, and it was completely mobile. The components included on the engine stand were, the engine, liquid fuel system, DAQ unit, and the gas analyzer. The engine was placed on a rubber block, and all electronics were placed on a board supported by anti-vibration rubber stand-offs to dampen unwanted vibrations. Casters were installed to make the entire unit mobile.

The control panel of the engine stand provides the user with complete control of the engine and displays live measurements. A laptop mounts to the panel and is used to record the data from the DAQ, tune the engine from the EcoCAL software, and display sensor measurements. An accurate lambda monitor (ALM) is mounted to the panel which displays the real time AFR of the engine, and can be calibrated for different fuels using the ALM GUI software. The panel also has a number of switches that control the fuel pump, spark, ECU power, and cylinder pressure transducer settings. There is a key switch for the electric starter, a potentiometer knob for throttle control, and an emergency stop button to disable power to the unit in the case of an emergency.

## 3.2 Design Summary

A summary of the experimental unit is provided below:

- The selected engine for the experimental unit was a single cylinder naturally aspirated 4-stroke SI engine. The engine is 0.208 L, has an 8.5:1 compression ratio and have an overhead valve arrangement.
- Ammonia and the combustion promoter (gasoline or heptane) are both introduced via port injection. Ammonia is injected using a gaseous fuel injector,

while gasoline or heptane are injected with a liquid injector. Both injectors are pressure regulated to 3 bar(g) and attached directly to the throttle body.

- A fully programmable Ecotrons ECU is used to control the fuel and ignition of the engine. The ECU is tuned using the speed density principal through EcoCAL software.

- An NI DAQ system is used to record and sync all incoming data. Microsoft Excel and MATLAB are used for post processing. In-cylinder pressure is mapped against crank angle with the use of a Kistler pressure transducer and BEI Sensors optical encoder. An EMS Gas five gas analyzer is used to measure $CO_2$, CO, $O_2$, HC, and $NO_2$ species.

- A mobile engine stand was developed to hold all of the experimental unit components, and to operate and control the engine from. The features of the stand include, live engine tuning abilities, live data display, fuel pump on/off, spark on/off, ECU on/off, cylinder pressure transducer settings, electric starter control, throttle control, and an emergency stop button. Additionally, vibration is dampened with a rubber block beneath the engine, and rubber stand-offs supporting the electronics board.

In Table 3.1 a summary of the technical specifications of the experimental unit is provided.

## 3.3 Limitations of Experimental Unit

At the time of writing, Canada and the rest of the world is in the midst of the unfortunate situation with the COVID-19 pandemic. This has resulted in a closure of the Ontario Tech University campus, meaning staff and students are not permitted access to any campus spaces, including labs. Consequently, the further refinement and development of the experimental unit has been restricted. While the developed experimental unit has great research capabilities, there are a few limitations with it's current status. Due to the unprecedented nature of this pandemic, a timeline for the return to campus is still unknown. These unforeseen circumstances and time limitations has forced this study to reach completion early. For this reason, the results presented in this study were taken during initial tests of the experimental unit that were not intended to be final. The limitations with the experimental unit and their effects on the results are as follows:

- The engine is operated under no engine load conditions. This has caused difficulties with engine tuning and controllability during tests, resulting in fluctuations in engine speed and lambda values. An engine dynamometer is required to address this issue and to allow for tuning of MBT timing and to determining knock limits. In this study the engine was reliably operated at fixed spark timings and low throttle positions. Data was only recorded during stable operation however, results are subject to fluctuations in engine speeds of $\pm 150$ RPM, and lambda of $\pm 0.05$. A small engine dynamometer was in development to address this issue.

- The AFR for blended fuels is unknown during testing. Due to limitations with the engine ECU, AFR for blended fuels could not be live monitored. The AFR is however determined during post-processing of the emissions data. A method for live monitoring was developed for future testing.

- The pressure sensor experiences scaling and calibration drift. Due to either the pressure sensor hardware or software, there has been changes in the scaling and calibration between tests. This has resulted in variations in pressure magnitude, and made the monitoring of cycle-to-cycle variation unreliable. For this reason, the results presented in this thesis are viewed as qualitative, rather than quantitative. This issue was under investigation prior to the campus closure.

- The engine does not have a fixed and controlled environment to operate. Tests have been conducted either in a climate controlled chamber or outdoors, depending on the fuels being tested and the facilities availability at the time of testing. This means there are variations in ambient conditions between some tests. A permanent engine testing room is in development.

Despite these limitations, it is important to note that the associated errors in the results will not have significant implications on the visible trends of the data. Considering the study data is viewed as a qualitative analysis, the results and trends are valid and in agreement with existing literature.

Table 3.1: Technical specifications of experimental unit

| Engine | |
|---|---|
| Engine Model | Pro.Point 208cc OHV Gas Engine |
| Engine Cycle | 4-stroke Otto Cycle |
| Number of Cylinders | 1 |
| Bore (mm) | 70.1 |
| Stroke (mm) | 54.1 |
| Displacement (L) | 0.208 |
| Compression Ratio | 8.5:1 |
| Ignition Method | SI |
| Exhaust After-treatment | None |

| Fuel System | |
|---|---|
| Types of Fuel | Liquid and Gaseous |
| Delivery Method | Port Injected for Both Fuels |
| Liquid Fuel Injector Flow Rate (g/min) | 80 |
| Liquid Fuel Pressure (bar(g)) | 3 |
| Liquid Fuel Tank Size (L) | 3.59 |
| Liquid Fuel Pump Rating (L/hr) | 166 |
| Gaseous Fuel Injector Flow Rate (g/min) | 45 |
| Gaseous Fuel Pressure (bar(g)) | 3 |
| Ammonia Tank Water Volume (L) | 126.29 |
| Ammonia Tank Pressure (bar(g)) | 7.86 |

| Engine Control Unit | |
|---|---|
| ECU Model | Ecotrons ECU-2T1C |
| Tuning Method | Speed Density |
| Trigger Input | Hall-effect |
| Ignition Type | Capacitor Discharge |
| Oxygen Sensor | Bosch LSU 4.9 |

| Data Acquisition | |
|---|---|
| DAQ Model | National Instruments |
| DAQ Software | NI LabVIEW 2019 |
| Cylinder Pressure Transducer Model | Kistler Model 6013CA |
| Charge Amplifier Model | Kistler Model 5073 |
| Cylinder Pressure Range (bar(a)) | 0-250 |
| Cylinder Pressure Sample Rate (Hz) | 2000 |
| Encoder Model | BEI Sensors H25 Optical Encoder |
| Encoder Resolution (ppr) | 720 |
| Exhaust Analyzer Model | EMS Gas 5-Gas Analyzer Model 5003 |
| Exhaust Species Measured | $CO_2$, CO, $O_2$, HC, and $NO_2$ |
| 5-Gas Analyzer Sample Rate (Hz) | 0.67 |

# Chapter 4

# Results and Discussion

In this chapter the experimental results are presented and the combustion and emission characteristics are analyzed. The chapter in divided into three sections. Section 4.1 provides an outline of the parametric analysis completed for this research. Section 4.2 analyzes the combustion characteristics and Section 4.3 analyzes the emission characteristics.

## 4.1 Parametric Analysis Outline

In order to understand the combustion and emission characteristics of ammonia blended fuels, a parametric analysis has been conducted. Table 4.1 shows the tests completed in this study. For baseline gasoline ($C_nH_{1.87n}$) and heptane ($C_7H_{16}$) tests, the effects of engine speed, lambda ($\lambda$), and spark timing are studied. For blended ammonia tests, blend ratio by mass ($NH_3$% – Hydrocarbon Fuel%), engine speed, and spark advance timing are studied. A variance of $\pm$150 RPM and $\pm$0.05 $\lambda$ is to be considered for these tests. Lambda tests and measurements were not conducted for blended cases in these tests. The $\lambda$ value for blended ammonia cases range from 0.87$\sim$1.21. A $\pm$3% variance is to be considered for fuel blend ratio.

For the ease of understanding, in Table 4.1 the Case ID follows the following naming convention, 'fuel_test#'. Where the fuel is either gasoline (G), heptane (H), or a gasoline/ammonia blend (GA). The tests are either engine speed (R), lambda (L), spark timing (ST), or fuel blend ratio (BR). Tests are numbered starting from 1, with the exception of GA_BR0 which starts at 0 because it is a baseline test with no blend.

The test conditions for each parameter were chosen such that a particular variable was tested through a range of commonly acceptable values, with all other variables

being held at a constant and reasonable mid-range value. For instance, in the engine speed tests for gasoline (G_R#) the engine speed was tested through a range starting from a minimum achievable speed to a maximum speed near the manufacturers recommended limit. A speed increment small enough to visibly see trends was used. The $\lambda$ value was set to an ideal value (stoichiometric), while spark timing was set to a common mid-range value ($15°bTDC$).

It should be noted that more tests were originally planned for this study to increase the number of data points and provide a clearer understanding of the combustion and emission trends. This however, was no possible due to the limitations discussed in Section 3.3. Unfortunately, for these same reasons, heptane/ammonia tests were not conducted. These tests were planned but were ultimately cancelled due to the COVID-19 pandemic. Baseline heptane tests were conducted however, and are compared to baseline gasoline tests to analyze its performance as a potential combustion promoter.

In the completed tests, 87 octane pump gasoline was utilized, which may contain up to 15% ethanol. Ethanol has a higher flame speed ($S_L$), and lower heating value than gasoline, so this may result in faster combustion with less heat energy for gasoline cases. Heptane was used opposed to n-heptane for the heptane tests. This may result in slight variances in some fuel properties in comparison to n-heptane. For tests with ammonia, 99.5% concentration anhydrous ammonia was used.

## 4.2 Combustion Characteristics

In this section, the combustion characteristics of a single average cycle per case are analyzed using in-cylinder pressure traces, heat release rate (HRR) traces, and required performance measurements. The performance measurements include, power, torque, specific fuel consumption ($SFC$), and combustion efficiency.

In-cylinder pressure traces used direct in-cylinder pressure and crank angle measurements. The HRR [J/°] was determined using Eq. 4.1 for apparent net HRR, and was plotted against crank angle for the HRR traces. In Eq. 4.1, $Q_n$ represents heat release [J], $\gamma$ is the specific heat ratio, $P$ is pressure [Pa], and $V$ is volume [$m^3$].

$$\frac{dQ_n}{d\theta} = \frac{\gamma}{\gamma - 1} P \frac{dV}{d\theta} + \frac{1}{\gamma - 1} V \frac{dP}{d\theta} \tag{4.1}$$

The mean effective pressure ($mep$) [Pa] was calculated by Eq. 4.2. Where $W$ is the indicated work per cycle [J], and $V$ is the displacement volume. $W$ is found using

Table 4.1: Outline of completed parametric analysis

Gasoline (Baseline)

| Case ID | Engine Speed (RPM) | Lambda ($\lambda$) | Spark Advance ($^\circ b$TDC) |
|---|---|---|---|
| G_R1 | 2000 | 1 | 15 |
| G_R2 | 3000 | | |
| G_R3 | 3500 | | |
| G_R4 | 4000 | | |
| G_R5 | 4500 | | |
| G_L1 | 3000 | 0.8 | 15 |
| G_L2 | | 1 | |
| G_L3 | | 1.1 | |
| G_L4 | | 1.2 | |
| G_ST1 | 3000 | 1 | 20 |
| G_ST2 | | | 15 |
| G_ST3 | | | 0 |

Heptane (Baseline)

| Case ID | Engine Speed (RPM) | Lambda ($\lambda$) | Spark Advance ($^\circ b$TDC) |
|---|---|---|---|
| H_R1 | 2200 | 1 | 15 |
| H_R2 | 3000 | | |
| H_R3 | 3500 | | |
| H_R4 | 4000 | | |
| H_R5 | 4400 | | |
| H_L1 | 3000 | 1 | 15 |
| H_L2 | | 1.1 | |
| H_L3 | | 1.2 | |
| H_ST1 | 3000 | 1 | 20 |
| H_ST2 | | | 15 |
| H_ST3 | | | 10 |
| H_ST4 | | | 5 |

Gasoline–Ammonia

| Case ID | Blend Ratio ($NH_3$% – Gasoline%) | Engine Speed (RPM) | Spark Advance ($^\circ b$TDC) |
|---|---|---|---|
| GA_BR0 | 0-100 | 4000 | 10 |
| GA_BR1 | 70-30 | | |
| GA_BR2 | 80-20 | | |
| GA_R1 | 70-30 | 2500 | 10 |
| GA_R2 | | 3000 | |
| GA_R3 | | 4000 | |
| GA_ST1 | 70-30 | 4000 | 20 |
| GA_ST2 | | | 10 |
| GA_ST3 | | | 0 |

an indicator diagram (pressure vs. volume) from cylinder pressure data.

$$mep = \frac{2W}{V} \tag{4.2}$$

Torque ($\tau$) [Nm] was calculated by Eq. 4.3.

$$\tau = \frac{mep \cdot V}{4\pi} \tag{4.3}$$

Power ($\dot{W}$) [kW] was calculated by Eq. 4.4. Where $N$ is engine speed [RPM].

$$\dot{W} = \frac{2\pi N\tau}{1000} \tag{4.4}$$

$SFC$ was calculated by Eq. 4.5. Where $\dot{m}_f$ is the mass flow rate of fuel [g/hr].

$$SFC = \frac{\dot{m}_f}{\dot{W}} \tag{4.5}$$

The combustion efficiency ($\eta_c$) was calculated by Eq. 4.6. Where $ppm_{HC,exhaust}$ is the volume of unburnt hydrocarbons in the exhaust [ppm], and $ppm_{HC,intake}$ is the volume of hydrocarbon fuel injected in the intake [ppm].

$$\eta_c = 1 - \frac{ppm_{HC,exhaust}}{ppm_{HC,intake}} \tag{4.6}$$

$ppm_{HC,intake}$ is taken directly from the emissions analyzer. $ppm_{HC,intake}$ is determined during post-processing using ECU and emissions data. It is worth noting that this analysis is only applied to hydrocarbon fuels, since ammonia slip was not measured in this study. For the purposes of this study $\eta_c$ is used to represent overall combustion efficiency.

In Section 4.2.3 and 4.3.3 the effects of $\lambda$ are examined. Lambda is the measure of how close an air fuel ratio (AFR) is to stoichiometric, as seen in Eq. 4.7. $AFR_{test}$ is the tested air fuel ratio, $AFR_{stoich}$ is the stoichiometric air fuel ratio, and $\phi$ is the equivalence ratio. Values below 1 are considered rich, and mean that there is excess fuel during combustion, and values above 1 are considered lean, which means there is excess air during combustion.

$$\lambda = \frac{AFR_{test}}{AFR_{stoich}} = \frac{1}{\phi} \tag{4.7}$$

### 4.2.1 Effects of Fuel Blend Ratio

The effects of ammonia to hydrocarbon blend ratio are explored here, where BR0 represents 100% gasoline, BR1 represents 70%-$NH_3$ and 30%-gasoline, and BR2 represents 80%-$NH_3$ and 20%-gasoline. It is important to restate that $\lambda$ was not controlled for blended tests. It was determined in post-processing that BR1 operated rich at $\lambda$ = 0.87 and BR2 operated lean at $\lambda$ = 1.12. BR0 was stoichiometric ($\lambda$ = 1). This is important because combustion and emission characteristics are a function of $\lambda$, and variances can have significant effects.

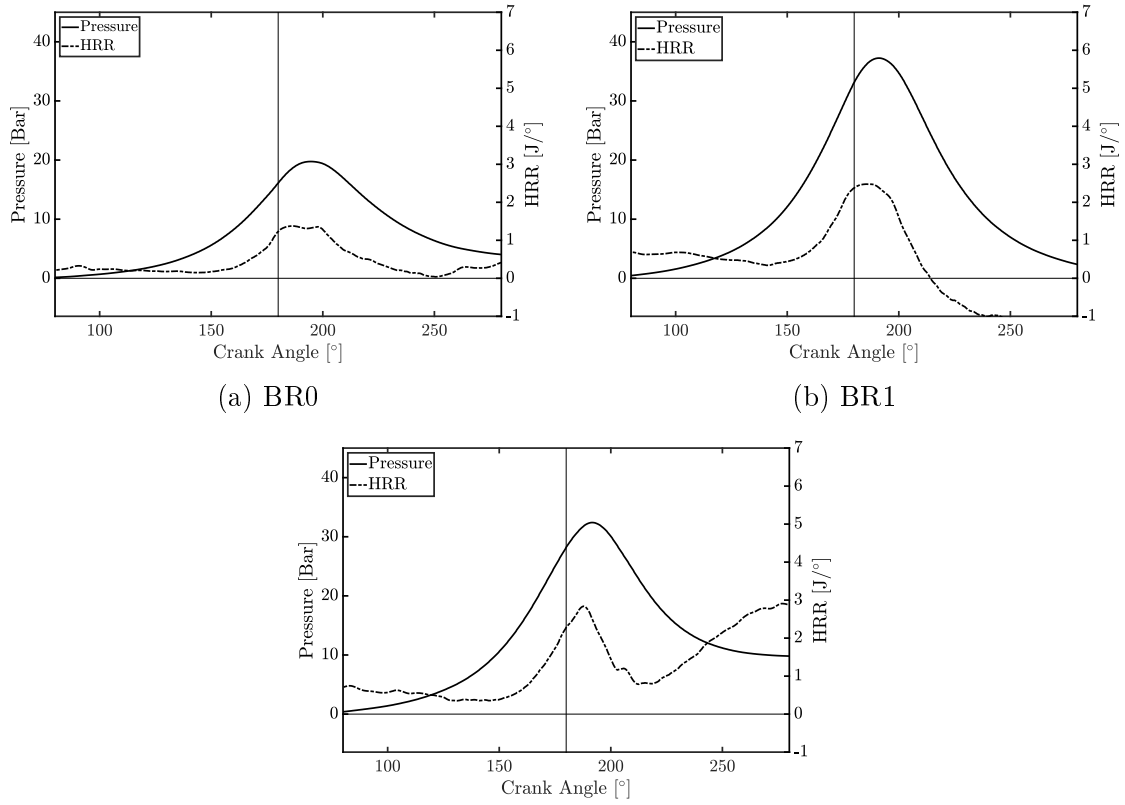


(a) BR0

(b) BR1

(c) BR2

Figure 4.1: Cylinder pressure and HRR vs. crank angle for different gasoline/$NH_3$ blend ratios. 4000 RPM, ST = 10° $b$TDC.

Figure 4.1 shows the pressure and HRR traces for the BR0, BR1, and BR2 fuel blend ratios. It can be seen that the peak cylinder pressures for the blended cases

have nearly double the cylinder pressure of BR0. This is because of the increased throttle position and fuel quantity injected from the ECU in dual fuel mode, which increases the available heat energy. It can also be seen that BR2 has a lower peak pressure than BR1, and carries a higher pressure in the exhaust. This characteristic is supported by the poor premixing of the fuels and oxidizer, resulting in lower ammonia $\eta_c$. The reduced $\eta_c$ is evident in the HRR trace, with the large heat rise in the power stroke of the cycle. It is hypothesized that the initial heat rise is from the combustion of gasoline, while the second one is from the combustion of ammonia. At this blend ratio and $\lambda$ value the fuels did not premix. Thus gasoline was combusted and it did not promote the combustion of ammonia well. The HRR of the BR0 and BR1 cases however, exhibit good premixed combustion characteristics. It is worth mentioning that the HRR in Figure 4.1b becomes negative after approximately 210° crank angle, this is a result of either heat transfer to the cylinder walls or drift associated with the cylinder pressure measurement. In the case of pressure measurement drift, the HRR profile still holds valid experiencing good premixed combustion.

It should also be noted that during testing the BR2 case was unable to achieve a stable engine operation like BR1. The engine operation for BR2 was erratic and the presence of ammonia slip could be smelt in the exhaust.

The performance measures are analyzed for each blend ratio. In Figure 4.2 the power ($\dot{W}$) and torque ($\tau$) with respect to blend ratio is presented. For the given engine speed and spark timing, it can be seen that both $\dot{W}$ and $\tau$ initially decrease with ammonia content until 70%. This can be attributed to a spark timing which is likely not suited for the lower flame speed ($S_L$) of ammonia. When ammonia content reaches 80% however, there is significant increase in $\dot{W}$ and $\tau$. This is because the two fuels exhibit poor micro-mixing prior to combustion. With 80% ammonia content, the ammonia combusts during the power stroke, thereby increasing cylinder pressure, $\tau$, and $\dot{W}$. This effect while resulting in increased $\dot{W}$ and $\tau$, also resulted in poor operating characteristics.

The specific fuel consumption ($SFC$) and combustion efficiency ($\eta_c$) for the blended ammonia cases can be seen in Figures 4.3a and 4.3b respectively. The $SFC$ shows to increase with ammonia content until 70% due to the increased amount of fuel used in the dual fuel system and reduced energy content of the blended fuel. More fuel mass is required to make comparable power to 100% gasoline. A low $SFC$ is good and representative of an efficient engine, as this means less fuel is required to make a single unit of power. The lower $SFC$ at 80% is due to the increase in $\dot{W}$, however this case is not representative of good combustion characteristics. In terms of $\eta_c$,

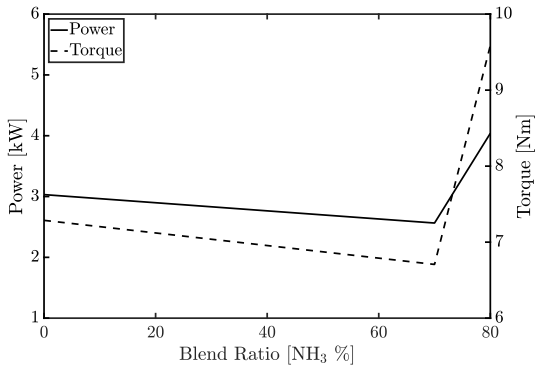


Figure 4.2: Power and torque vs. $NH_3$ blend ratio. 4000 RPM, ST = 10° $b$TDC.

it can be seen that ammonia content lowers the $\eta_c$. This may be a result of a rich mixture, a sub-optimal fuel blend ratio, or poor premixing of fuels. At 80% ammonia content the $\eta_c$ is comparable to 0% ammonia. This is because $\eta_c$ is measured from unburnt hydrocarbon emissions, and is not fully representative of ammonia $\eta_c$. In the BR2 case, it is believed that the gasoline combusts almost completely and then the ammonia combustion begins. During testing it was evident that the ammonia $\eta_c$ was much lower and ammonia slip occurred. For these reasons, only the BR1 ratio was utilized in the remainder of the tests and the BR2 case was not tested.

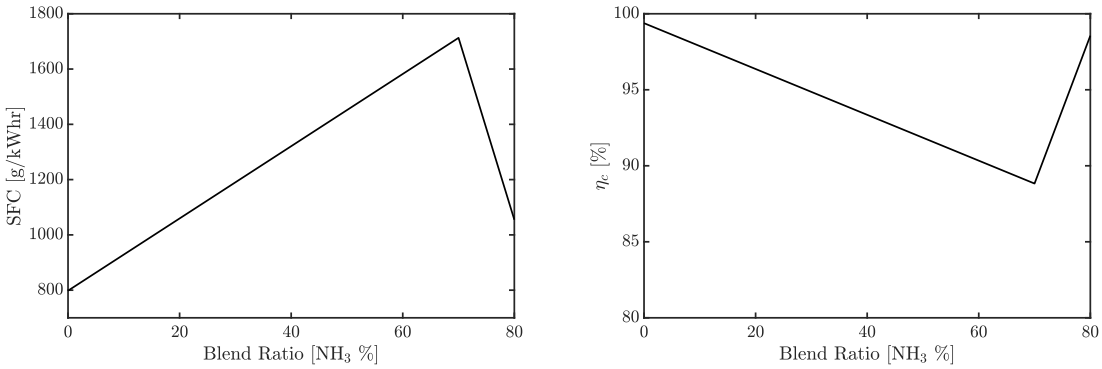


(a) SFC (b) Combustion efficiency

Figure 4.3: SFC and combustion efficiency vs. $NH_3$ blend ratio. 4000 RPM, ST = 10° $b$TDC.

### 4.2.2 Effects of Engine Speed

#### 4.2.2.1 Baseline Cases

Pressure and HRR traces of the baseline 100% gasoline and 100% heptane have been plotted to analyze the characteristics of the baseline fuels prior to blending. The

pressure and HRR traces at different engine speeds are shown in Figure 4.4 and Figure 4.5 for gasoline and heptane respectively. These figures show that as engine speed increases, both the pressure and HRR increase, and that both fuels exhibit similar magnitudes of pressure. These trends are expected since fuel mass increases with engine speed, increasing the available heat energy.

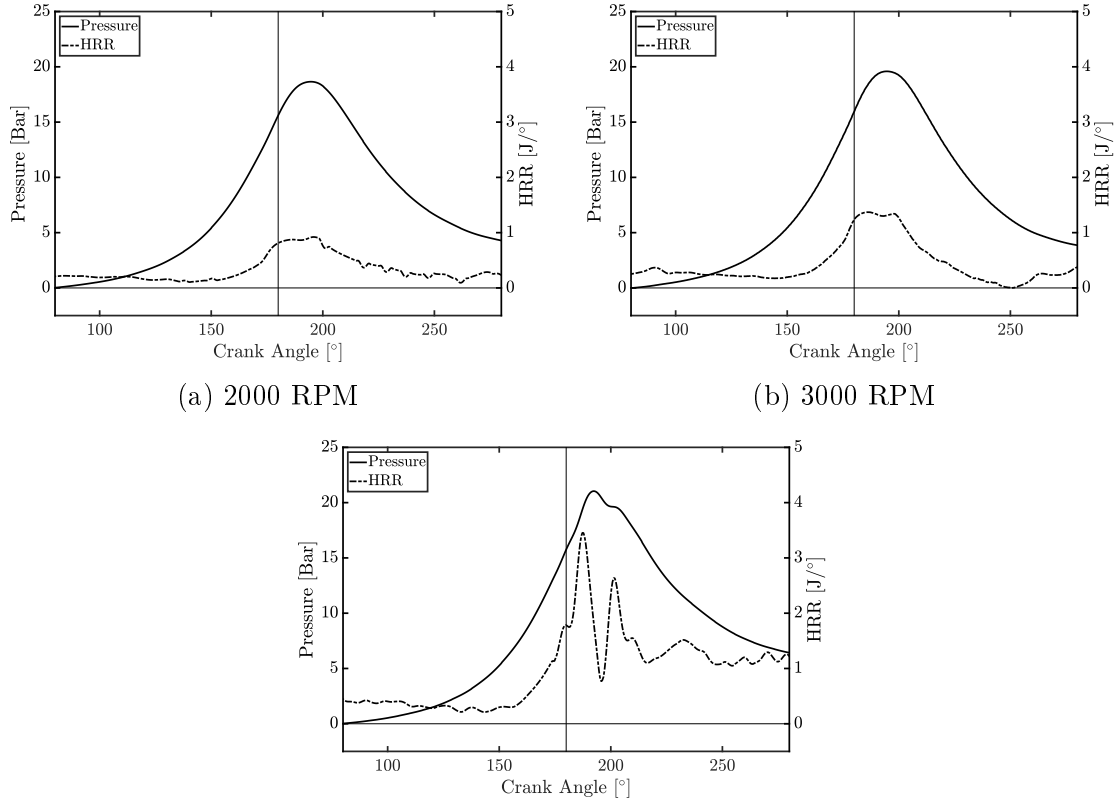


(a) 2000 RPM

(b) 3000 RPM

(c) 4000 RPM

Figure 4.4: Cylinder pressure and HRR vs. crank angle for 100% gasoline at different engine speeds. $\lambda = 1$, ST = 15° $b$TDC.

In Figure 4.4c, at 4000 RPM for the gasoline case, the HRR trace shows two spikes in heat release from approximately 180° to 210°. This effect is attributed to diffusion flames occurring, opposed to premixed flames. In diffusion flames the fuel and oxidizer are non premixed, and the burning rate becomes dependent on the rate at which the fuel and oxidizer come together. This phenomenon is not desirable in SI engines as the combustion duration increases, decreasing combustion efficiency, and increasing overall combustion temperatures and $NO_x$ levels. The diffusion flames in this particular case can be a result of the low throttle position creating high intake restriction and inhibiting the premixing of fuel and oxidizer. In may also be an indication that the fuel injection timing or design needs to be improved to enhance

premixing. As engine speeds increase, premixing time decreases, so injection strategies must be suited to accommodate this factor. Similar results can be seen in Figure 4.5 for heptane cases, however it is a less extreme example of diffusion flames. This result may be due to a slower mass diffusivity to thermal diffusivity of heptane.

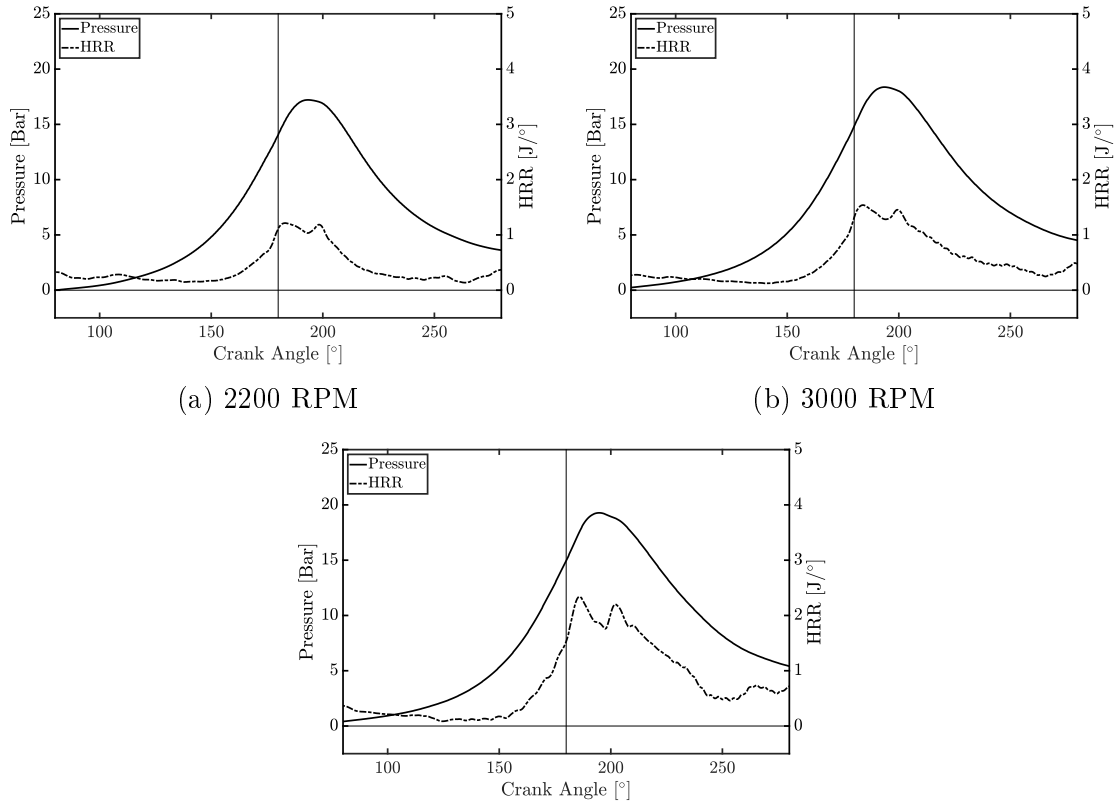


(a) 2200 RPM

(b) 3000 RPM

(c) 4000 RPM

Figure 4.5: Cylinder pressure and HRR vs. crank angle for 100% heptane at different engine speeds. $\lambda = 1$, ST = 15° $b$TDC.

The performance measures of the engine with respect to engine speed are now examined for the two baseline fuels. Figure 4.6 shows $\dot{W}$ and $\tau$ as a function of engine speed for gasoline and heptane. It can be seen that overall $\dot{W}$ and $\tau$ trends and magnitudes for both fuels show similar effects. This is expected since gasoline and heptane have similar energy content for stoichiometric masses of fuel. The two fuels are near identical during mid range engine speeds, however gasoline shows higher $\dot{W}$ and $\tau$ at both low and high engine speeds. This is due to the fixed spark timing of the engine. Neither fuel is tuned for MBT timing, so it is likely that the spark timing of 15° $b$TDC is better suited for gasoline than heptane. Analysis of this topic is further discussed in Section 4.2.4.1.

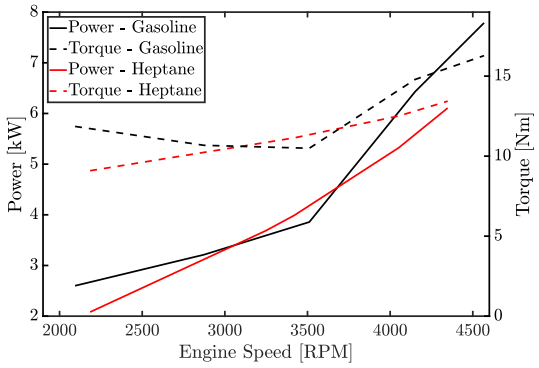


Figure 4.6: Power and torque vs. engine speed for 100% gasoline and 100% heptane. $\lambda = 1$, ST = 15° $b$TDC.

Figures 4.7a and 4.7b show the $SFC$ and $\eta_c$ respectively for the two baseline fuels as a function of engine speed. Both fuels exhibit similar magnitudes and trends in both $SFC$ and $\eta_c$. $SFC$ trends downward since volumetric, combustion, and thermal efficiencies tend to increase with engine speed. The $\eta_c$ increases with engine speed due to increased premixing and heat.

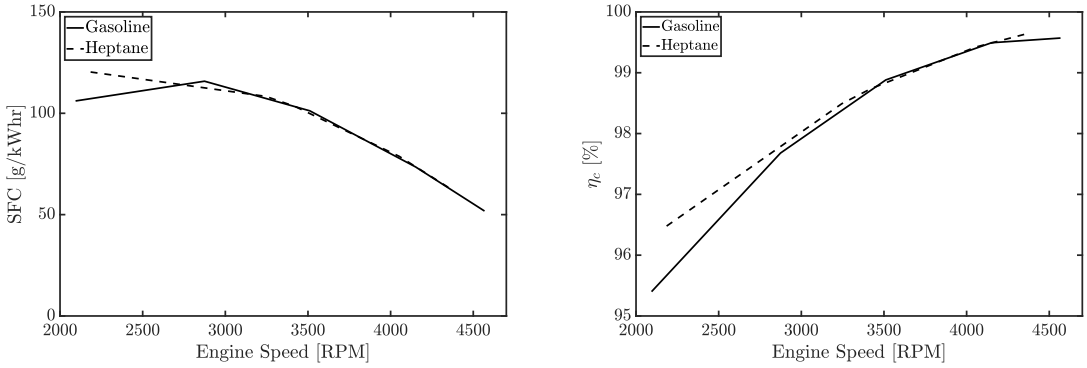


(a) SFC

(b) Combustion efficiency

Figure 4.7: SFC and combustion efficiency vs. engine speed for 100% gasoline and 100% heptane. $\lambda = 1$, ST = 15° $b$TDC.

#### 4.2.2.2 Blended Ammonia Cases

The effect of engine speed with gasoline/ammonia blend is examined and discussed here. In Figure 4.8 the pressure and HRR traces are shown for the BR1 case. Similar to Section 4.2.1, it can be seen that the cylinder pressures for BR1 is higher than the baseline cases (Figures 4.4 and 4.5); approximately 50% higher in these tests. This increase in cylinder pressure is due to the increased fuel quantity and the available heat energy. The figure also shows that the HRR profiles are smoother than both

baseline cases, as a result of good premixing taking place between the two fuels and oxidizer prior to combustion. The increased fuel quantity and enhanced micro-mixing characteristics of gaseous ammonia for this blend ratio are the primary causes of this.

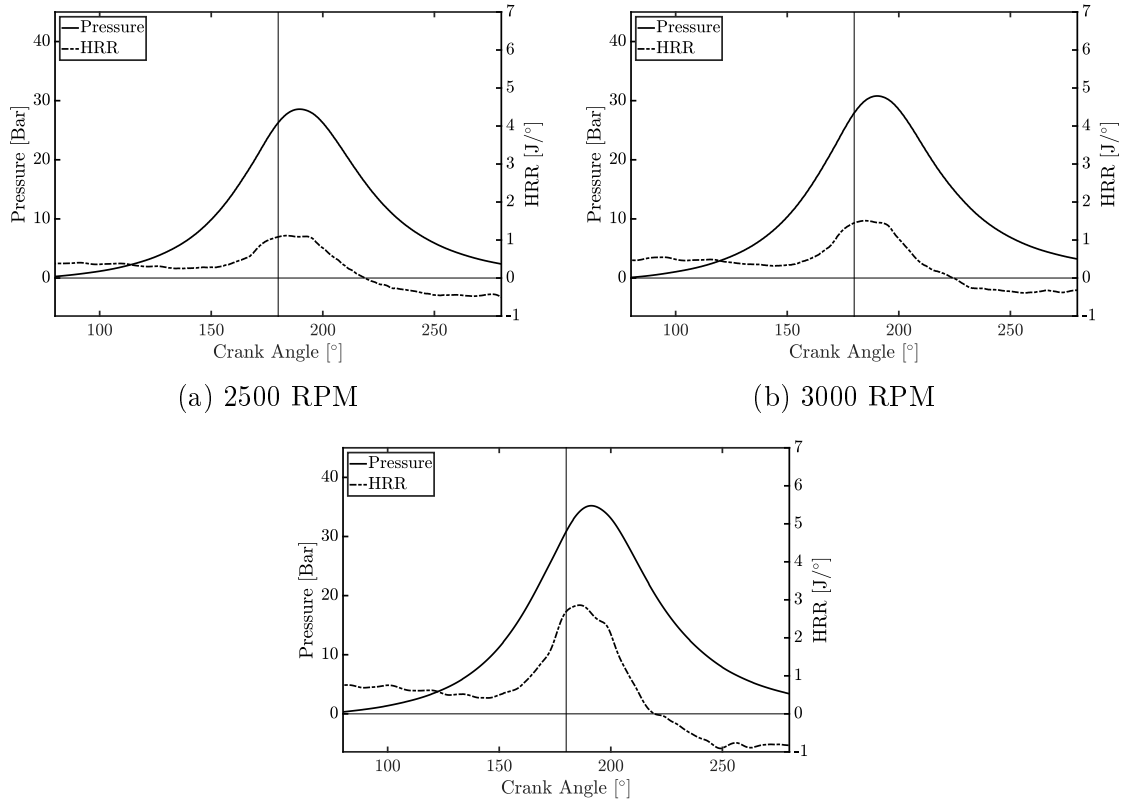


(a) 2500 RPM

(b) 3000 RPM

(c) 4000 RPM

Figure 4.8: Cylinder pressure and HRR vs. crank angle for BR1 at different engine speeds. ST = 10° $b$TDC.

The $\dot{W}$ and $\tau$ of the BR1 and BR0 cases are shown in Figure 4.9. The BR1 case is set to a fixed spark timing of 15° $b$TDC and the BR0 case is set to 10° $b$TDC. It can be seen that the overall $\dot{W}$ and $\tau$ of BR1 is lower than BR0 in all instances. This can be expected by the lower spark timing used in the BR1 case. The $\tau$ of BR1 peaks at approximately 2900 RPM, where as BR0 is continuing to rise at 4500 RPM. Since ammonia has a lower $S_L$, the combustion duration is longer for BR1, and more spark advance is necessary to achieve best torque. If the engine were tuned to MBT timing, the overall $\dot{W}$ and $\tau$ of BR1 would improve, and the location of peak $\tau$ would likely shift higher in the speed range.

As seen previously, BR1 exhibits significantly higher $SFC$ than BR0, as seen in Figure 4.10a. This is because of the increased fuel mass per cycle with decreased

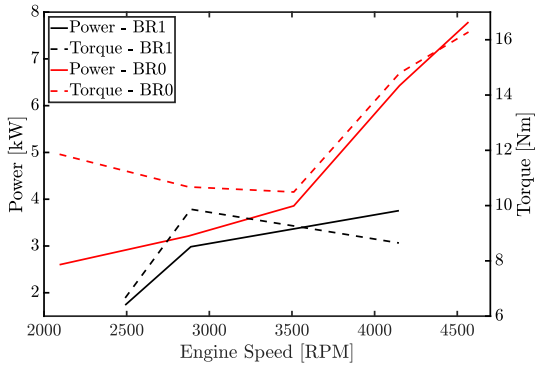


Figure 4.9: Power and torque vs. engine speed for BR0 and BR1. ST = 15° $b$TDC for BR0 and ST = 10° $b$TDC for BR1.

energy content in the blended fuel. The $SFC$ is lowest around 3000 RPM because this is the approximate location of peak $\dot{W}$ and $\tau$. The $\eta_c$ is shown in Figure 4.10b for BR1 and BR0. From this figure it is evident that the ammonia content lowers the $\eta_c$ by approximately 8% at lower engine speeds. At higher engine speeds this lowers to about 4% due to improved mixing at high engine speeds.

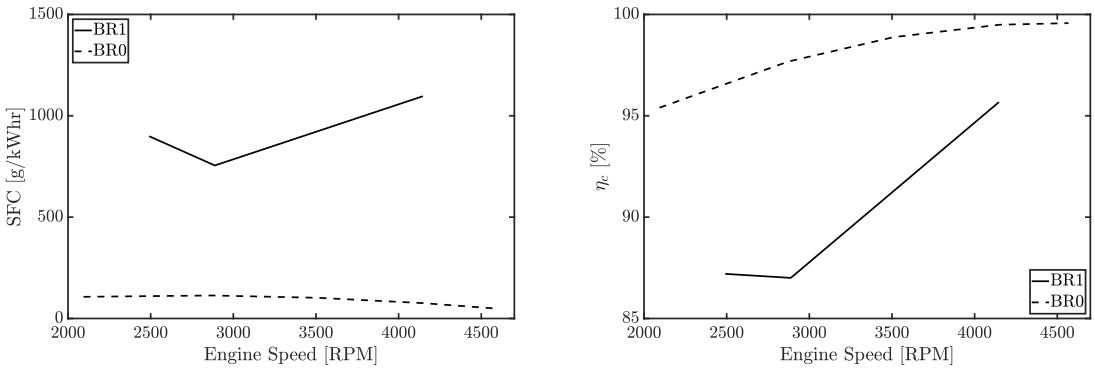


(a) SFC (b) Combustion efficiency

Figure 4.10: SFC and combustion efficiency vs. engine speed for BR0 and BR1. ST = 15° $b$TDC for BR0 and ST = 10° $b$TDC for BR1.

### 4.2.3 Effects of Air Fuel Ratio (Lambda)

The effects of $\lambda$ are explored for the two baseline fuel cases. For 100% gasoline the pressure and HRR traces are shown in Figure 4.11. The cylinder pressure traces show that as $\lambda$ increases from rich to lean (L1 to L4) the cylinder pressure decreases. This effect is attributed to the decreased mass of fuel utilized in lean mixtures. The HRR for the rich mixture L1 exhibits good premixed combustion up to approximately

210° and then excess fuel is burned through diffusion combustion, where as the stoichiometric mixture L2 has good premixed combustion throughout due to its ideal mixture. The two lean cases, L3 and L4, show the occurrence diffusion combustion due to reduced premixing. With less fuel present in the air stream, mass diffusion is not high enough for good premixing. Heptane shows similar pressure and HRR trends in Figure 4.12.

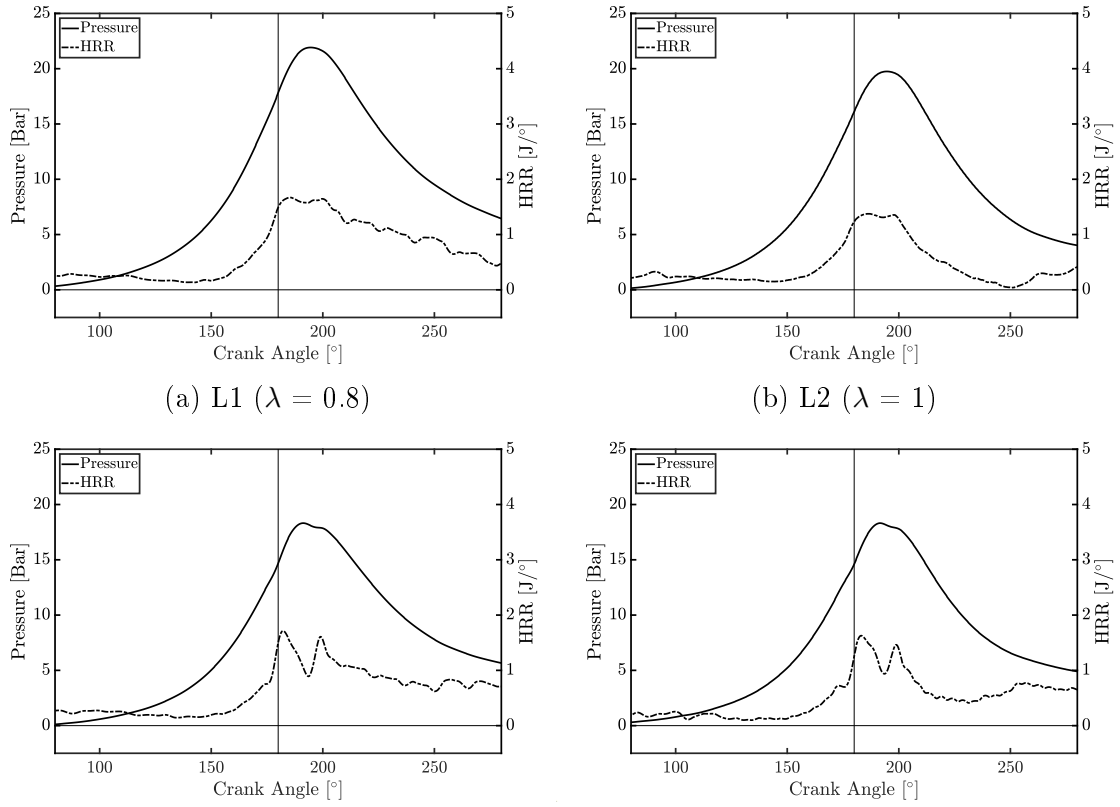


(a) L1 ($\lambda = 0.8$)

(b) L2 ($\lambda = 1$)

(c) L3 ($\lambda = 1.1$)

(d) L4 ($\lambda = 1.2$)

Figure 4.11: Cylinder pressure and HRR vs. crank angle for 100% gasoline at various lambda values. 3000 RPM, ST = 15° $b$TDC.

With respect to $\lambda$, the $\dot{W}$ and $\tau$ for both fuels follow predictable trends, as seen in Figure 4.13. It is evident that as fuel mixtures get richer, both $\dot{W}$ and $\tau$ increase due to increased fuel content, and higher $S_L$ for rich mixtures. Heptane produces lower $\dot{W}$ and $\tau$ than gasoline in all instances likely due a spark timing that favours gasoline over heptane for the given engine speed.

As seen in Figure 4.14a the $SFC$ for heptane follows the same trend as gasoline, but with about a 4∼10% increase in magnitude overall. This increase in $SFC$ is associated to the difference in ideal spark timing between the two fuels. In these tests

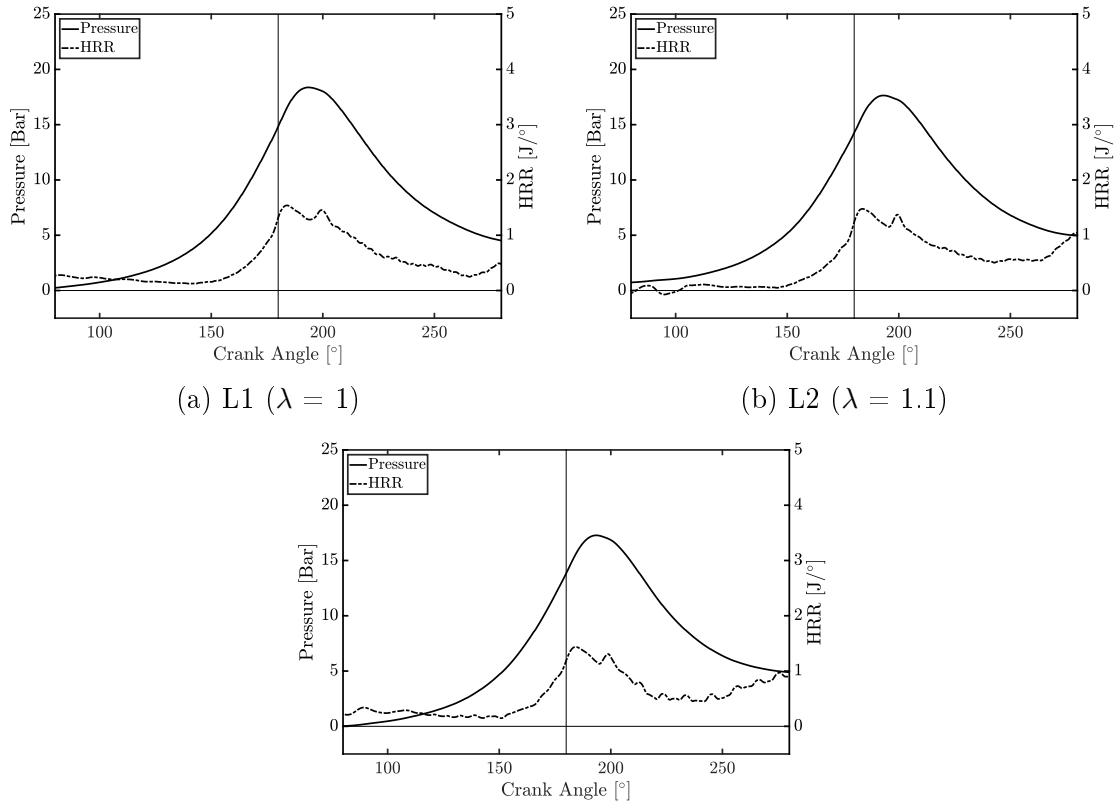


(a) L1 ($\lambda = 1$)

(b) L2 ($\lambda = 1.1$)

(c) L3 ($\lambda = 1.2$)

Figure 4.12: Cylinder pressure and HRR vs. crank angle for 100% heptane at various lambda values. 3000 RPM, ST = 15° $b$TDC.

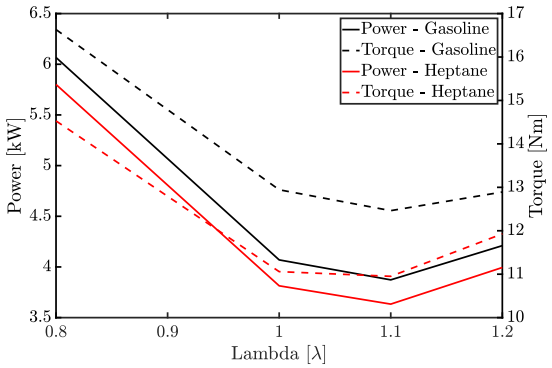


Figure 4.13: Power and torque vs. lambda for 100% gasoline and 100% heptane. 3000 RPM, ST = 15° $b$TDC. 0.8 to 1 $\lambda$ for heptane is determined via polyfit.

heptane produces less $\dot{W}$ for the given spark timing, resulting in lower $SFC$. The $\eta_c$ for gasoline and heptane are near identical, with a variance of 0.3 $\sim$ 0.5%, and heptane being higher in all cases. $\eta_c$ increases as mixtures get leaner because less fuel is being injected and there is more oxygen present for the fuel to consume.

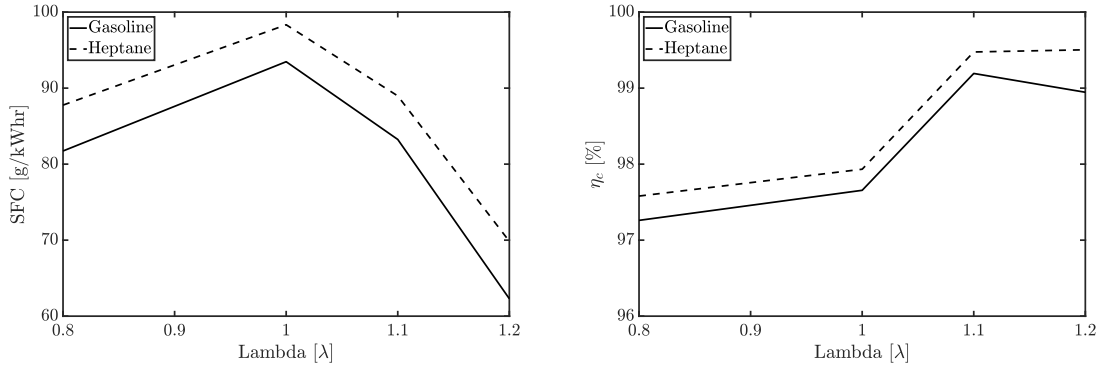


(a) SFC (b) Combustion efficiency

Figure 4.14: SFC and combustion efficiency vs. lambda for 100% gasoline and 100% heptane. 3000 RPM, ST = 15° $b$TDC. 0.8-1 $\lambda$ for heptane is determined via polyfit.

### 4.2.4 Effects of Spark Timing

#### 4.2.4.1 Baseline Cases

The effects of spark timing are analyzed for the baseline fuels. In Figure 4.15 the $\dot{W}$ and $\tau$ against spark timing are shown. From this figure it is clear that gasoline and heptane perform best at different spark timings as previously discussed. Gasoline has highest $\dot{W}$ and $\tau$ at -15° $b$TDC, while heptane has highest $\dot{W}$ and $\tau$ at -10° $b$TDC. It was expected that heptane would have peak $\dot{W}$ and $\tau$ at a slightly more advanced spark angle than gasoline however, because of the lower $S_L$ of heptane (see Table 1.1) increasing combustion duration. This outcome is due to variances in fuel properties, as mentioned in Section 4.1.

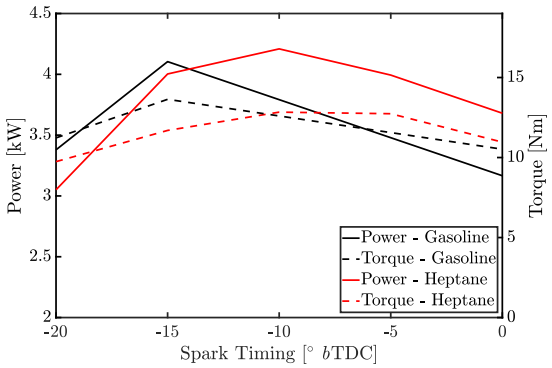


Figure 4.15: Power and torque vs. spark timing for 100% gasoline and 100% heptane. 3000 RPM, $\lambda$ = 1. -5 to 0° $b$TDC for heptane is determined via polyfit.

The *SFC* for these fuels with respect to spark timing have similar trends, but

are phased about 10° apart, as seen in Figure 4.16a. For heptane, $SFC$ gradually decreases as spark advance is decreased to -5° $b$TDC. After this point $SFC$ begins to increase, because of the increased power levels for heptane at low spark timing. Gasoline however, decreases as spark timing is decreased until only -15° $b$TDC, and increases after this point. This trend is expected as $SFC$ generally tends to reach a minimum around the same location as peak torque.

The $\eta_c$ for gasoline and heptane with respect to spark timing, is shown in Figure 4.16b. Both fuels trend upward as spark advance timing is decreased, and are within 1% of each other. Similar to the $\dot{W}$ in Figure 4.15, heptane outperforms gasoline at spark advance angles below -15° $b$TDC.

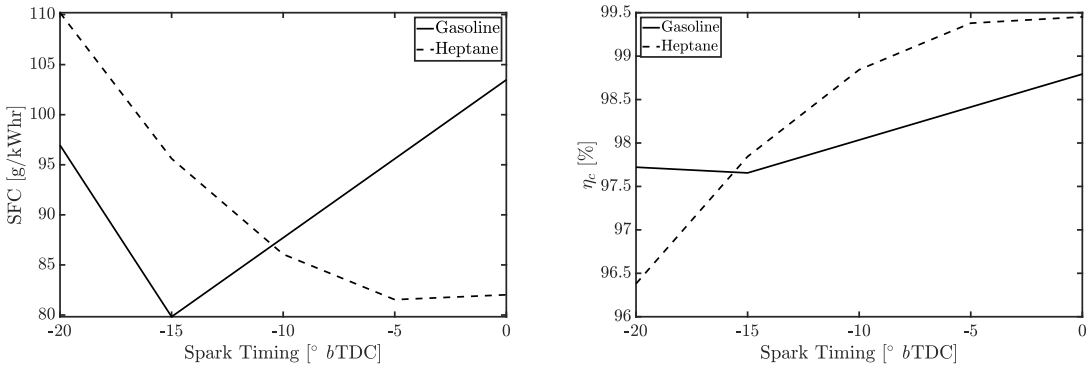


(a) SFC (b) Combustion efficiency

Figure 4.16: SFC and combustion efficiency vs. spark timing for 100% gasoline and 100% heptane. 3000 RPM, $\lambda = 1$. -5 to 0° $b$TDC for heptane is determined via polyfit.

#### 4.2.4.2 Blended Ammonia Cases

The effects of spark timing on blended ammonia fuels are analyzed. The $\dot{W}$ and $\tau$ of BR1 and BR0 cases are presented in Figure 4.17. It can be seen that at -15° $b$TDC the $\dot{W}$ of BR1 and BR0 are similar. As spark advance is decreased past this point, BR0 has better $\dot{W}$ and $\tau$, but if spark advance is increased, the $\dot{W}$ of BR1 exceeds BR0 and the $\tau$ exceeds BR0 after about -19° $b$TDC. For BR1, spark advance higher than -10° $b$TDC results in a significant increase in both $\dot{W}$ and $\tau$. This outcome is a result of the increased combustion duration of BR1, due to the slower $S_L$ of ammonia. A key take away from this figure is that more spark advance is required for blended ammonia fuels to see comparable $\dot{W}$ and $\tau$ than pure gasoline.

As observed in the engine speed cases, the spark timing cases for BR1 also has increased $SFC$ and decreased $\eta_c$. This can be seen from Figures 4.18a and 4.18b for

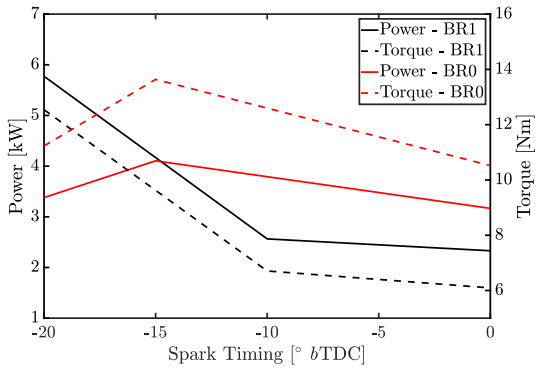


Figure 4.17: Power and torque vs. spark timing for BR0 and BR1. 3000 RPM for BR0 and 4000 RPM for BR1.

$SFC$ and $\eta_c$ respectively. In terms of $SFC$, the overall fuel consumption of BR1 is greater than BR0, however as spark timing advances, the $SFC$ significantly improves as power levels increase. It is evident from Figure 4.18a that more advanced spark timing should be explored to achieve improved $SFC$ in the BR1 case. The $\eta_c$ for BR1 is improved at -10° $b$TDC as a result of decreased power, increased throttle, and improved mixing.

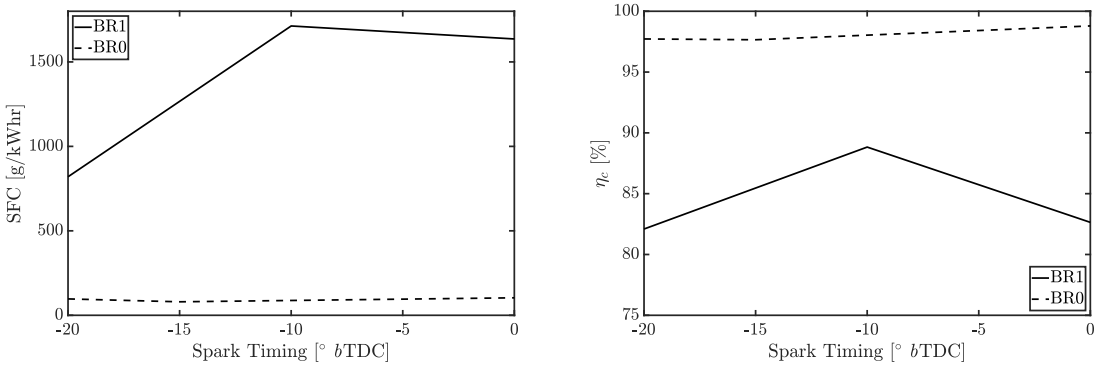


(a) SFC (b) Combustion efficiency

Figure 4.18: SFC and combustion efficiency vs. spark timing for BR0 and BR1. 3000 RPM for BR0 and 4000 RPM for BR1.

### 4.2.5 Effects of Cycle-to-Cycle Variation

In a typical SI engine cycle-to-cycle variation is a common occurrence due to variations in mixture motion and composition [10]. This can result in peak pressure variations between cycles in the order of ∼10 bar or more for a given engine [10]. As mentioned in Section 3.3 the monitoring of cycle-to-cycle variation in this study was unreliable

due to drift experienced by the in-cylinder pressure measurement. The resulting cycle-to-cycle variation for a given gasoline/ammonia case (GA_BR1) is shown in Figure 4.19. As seen by the error bars in the figure there is a variation range of about 1∼3 bar around peak pressure for 70 consecutive engine cycles. Similar variation was observed in all baseline and blended cases.

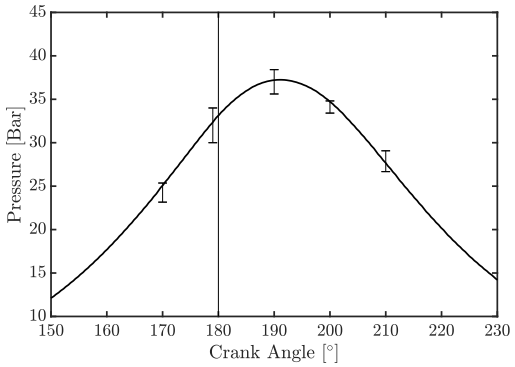


Figure 4.19: Cycle-to-cycle variation for 70 consecutive engine cycles in case GA_BR1.

### 4.2.6 *Section Summary*

The results presented in this section showed that gasoline/ammonia blends exhibit good premixed combustion characteristics when limited to 70% $NH_3$ content (BR1 case). This is due to good micro-mixing characteristics at this fuel blend ratio. It was seen that gasoline and heptane performed similarly overall, and that heptane required less spark advancement because of its lower flame speed, which is advantageous for an ammonia combustion promoter. $SFC$ for the BR1 cases were significantly higher due to the increased air flow and fuel mass injected, as well as decreased energy from the blended fuel. $\eta_c$ was lower for BR1 cases due to either insufficient premixing or a sub-optimal fuel blend ratio, however $\eta_c$ increases with engine speed due to improved premixing. Gasoline/ammonia blends require high spark advancements to see improved combustion characteristics. This is because of the extended combustion duration due to slow flame speeds. In the next section the emission characteristics of these tests are presented.

## 4.3 Emission Characteristics

In this section the emission characteristics are examined and discussed using data collected from a five gas emissions analyzer. The analyzer measures carbon dioxide

($CO_2$), carbon monoxide (CO), oxygen ($O_2$), unburnt hydrocarbons (HC), and nitrogen dioxide ($NO_2$) exhaust species. $CO_2$, CO, and $O_2$ are measured in [%], and HC and $NO_2$ are measured in [ppm]. All species are measured with respect to volume. It is important to note that ammonia slip was not monitored in this study and no exhaust after treatment devices were used.

Similar to Section 4.2 this section will study the effects of ammonia to hydrocarbon fuel blend ratio, engine speed, lambda ($\lambda$) and spark timing. It is worth noting that emissions are known to have a strong correlation to air fuel ratio (AFR), or $\lambda$. For typical IC engine applications, gasoline fueled engines generally follow the emission trends as shown in Figure 4.20. It can be seen that $CO_2$ peaks near stoichiometric conditions (solid black bar in figure), as the ideal AFR means the correct proportion of fuel and oxidizer are ingested to be fully consumed during combustion. Figure 4.20 shows that HC decreases as AFR becomes leaner and excess fuel quantity reduces, resulting in higher $\eta_c$. Moreover, HC increases at excessively lean mixtures due to reduced heat and premixing. The CO significantly declines as AFR becomes lean and excess $O_2$ increases. The $NO_x$ emissions peak under slightly lean conditions due to high cylinder temperatures. It is desirable to keep $CO_2$, CO, HC, and $NO_2$ species low, as they impose negative environmental and health impacts.

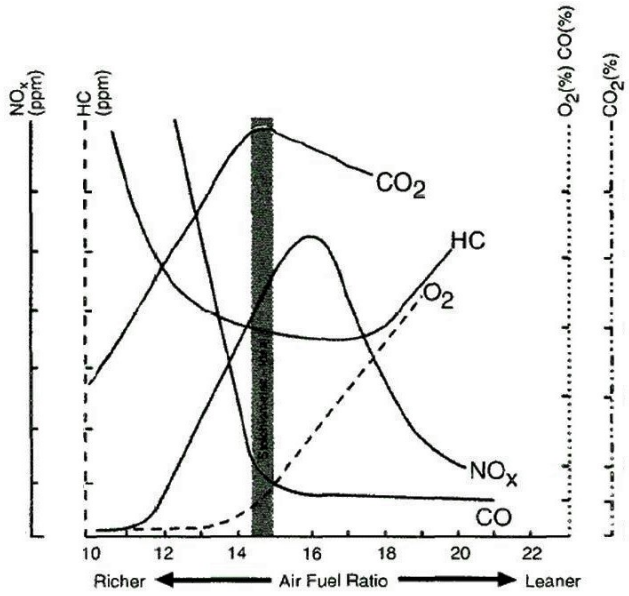


Figure 4.20: Emissions as a function of AFR in a gasoline fueled SI engine. (Taken and adapted from [47]).

### 4.3.1 Effects of Fuel Blend Ratio

The exhaust emissions in [%] and [ppm] for the fuel blend ratio cases BR0, BR1, and BR2, are presented in Figure 4.21a. From Figure 4.21a it can be seen that all species appear to increase with higher ammonia content, which is undesirable. This characteristic is a product of two factors.

(1) The throttle position was higher for blended fuels in conducted tests, resulting in increased air flow. The increased air flow automatically increases fuel injection by the ECU. This results in higher emissions due to higher fuel consumption rates per cycle. To analyze this further, data has been plotted in [g/kWhr] in Figure 4.21b. This makes emissions species specific to power output and the cases more comparable. From 4.21b it can be seen that as ammonia content increases to 70%, $CO_2$ decreases, CO increases, HC increases, and $NO_2$ increases. Ammonia content higher than 70%, the $CO_2$ increases, CO decreases, and HC decreases. As discussed in Section 4.2.1 ammonia content higher than 70% has adverse effects on combustion and operating characteristics.

(2) All three cases operated at different $\lambda$ values. BR0 operated at stoichiometric ($\lambda = 1$), BR1 operated rich ($\lambda = 0.87$), and BR2 operated lean at ($\lambda = 1.12$). Since emissions are strongly correlated to $\lambda$ this has a significant role on the outcome. Thus the increased CO and HC emissions at 70% ammonia content are a result of a rich AFR.

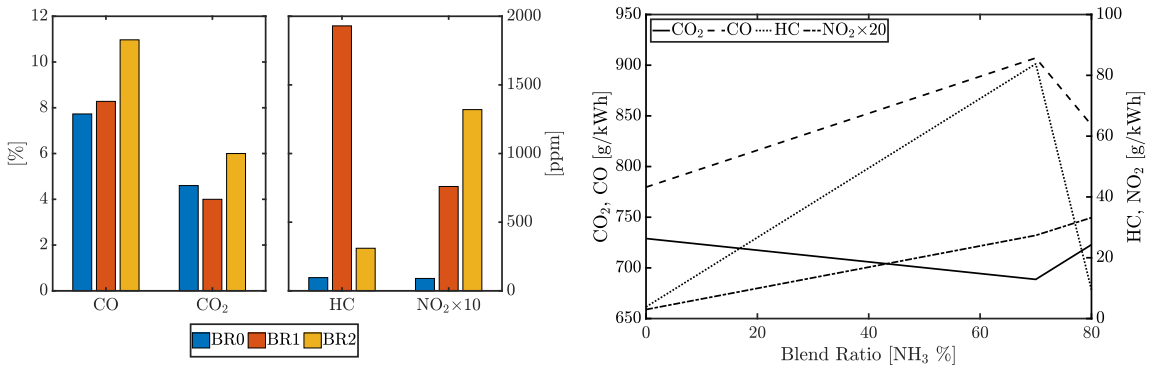


(a) [% and ppm] (b) [g/kWhr]

Figure 4.21: Emissions vs. $NH_3$ blend ratio. 4000 RPM, ST = 10° $b$TDC.

### 4.3.2 Effects of Engine Speed

#### 4.3.2.1 Baseline Cases

The emissions as a function of engine speed is presented and explored here. Figure 4.22a and Figure 4.22b show the emissions for gasoline and heptane respectively. Both fuels exhibit similar trends with respect to engine speed. The emission species CO trends downward, $CO_2$ trends upward, HC trends downward, and $NO_2$ trends upward. These trends are associated to improved premixing and combustion characteristics with increased engine speed. Complete premixed stoichiometric combustion results in low CO and HC levels, and high $CO_2$. This is because under stoichiometric conditions, the fuel and oxidizer are fully consumed during combustion and only produce $CO_2$ and $H_2O$. The emission species $NO_2$ is a function of gas temperature; high temperature results in high $NO_2$. As seen from Figures 4.22a and 4.22b, increased engine speed brings the emissions closer to the complete premixed stoichiometric scenario. In Figure 4.22a the $NO_2$ in case R1 does not fit within the upward trend, as these results are high for the particular cycle running at 2000 RPM. Therefore cycle-to-cycle variation can play a pivotal role here.

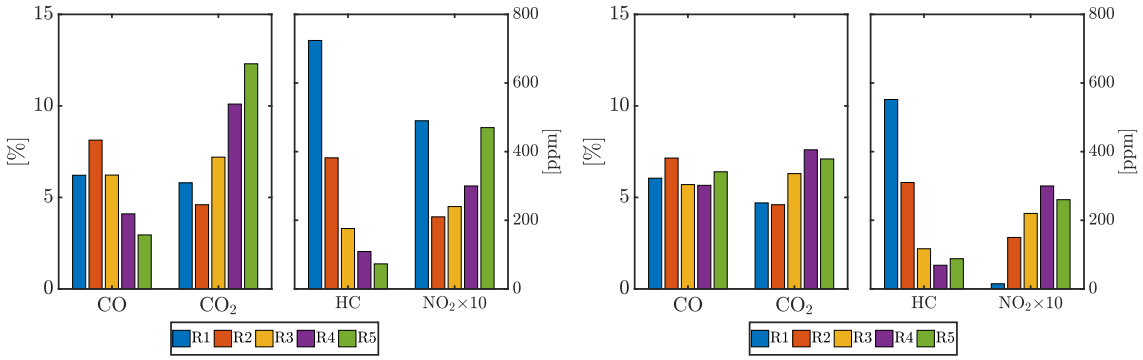


(a) Gasoline (b) Heptane

Figure 4.22: Emissions vs. engine speed for 100% gasoline and 100% heptane. $\lambda = 1$, ST = 15° $b$TDC.

Figure 4.23 shows a comparison between gasoline and heptane as a function of engine speed. Both fuels operated at similar throttle positions, therefore the [% and ppm] results are more comparable between the fuels. From Figure 4.23a it can be seen that heptane produces less $CO_2$ than gasoline, especially at higher engine speeds. The CO for gasoline declines with engine speed, however CO for heptane remains consistent across the speed range. At approximately 3700 RPM and higher, gasoline

produces less CO in comparison to heptane. The HC and $NO_2$ exhibit similar trends with increasing engine speeds for both fuels. Such trends are because of the fixed spark timing between the fuels. As discovered in Section 4.2.4.1, gasoline operates better at higher spark advance than heptane for a given engine speed. At higher engine speeds the spark timing is better suited for gasoline, resulting in improved combustion characteristics. When these two fuels are compared in units [g/kWhr], they are showing similar trends and magnitudes, because of their similar chemical compounds and fuel properties. At higher engine speeds, gasoline does produce higher $CO_2$ levels, but this is due to the combustion characteristics of heptane at 15° $b$TDC spark advance.

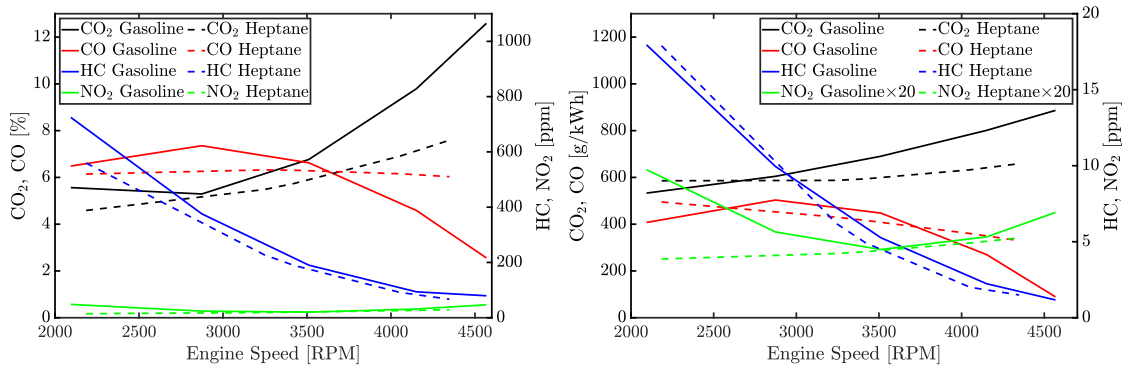


(a) [% and ppm] (b) [g/kWhr]

Figure 4.23: Emissions vs. engine speed for 100% gasoline and 100% heptane. $\lambda = 1$, ST = 15° $b$TDC.

#### 4.3.2.2 Blended Ammonia Cases

In Figure 4.24 the emissions as a function of engine speed is presented for the BR1 case. It can be seen that all emissions other than HC shows an upward trend with engine speed for the gasoline/ammonia blend. This is different than the baseline cases, where CO trends downward with engine speed. This phenomenon is attributed to the BR1 case operating at a richer AFR, increasing CO emissions. The HC emissions in this test increase at case R2 (4000 RPM), this however is due to increased fuel content, while combustion efficiency remains consistent at this engine speed (seen in Figure 4.10b).

Figure 4.25 compares the BR0 and BR1 fuel blend ratio cases in [% and ppm] and in [g/kWhr]. Figure 4.25a shows that, BR0 and BR1 follow different trends for CO emissions due to the variation in $\lambda$ value, but all other emissions follow similar trends. A key feature seen in this figure is the nearly 4% volume decrease in $CO_2$ emissions

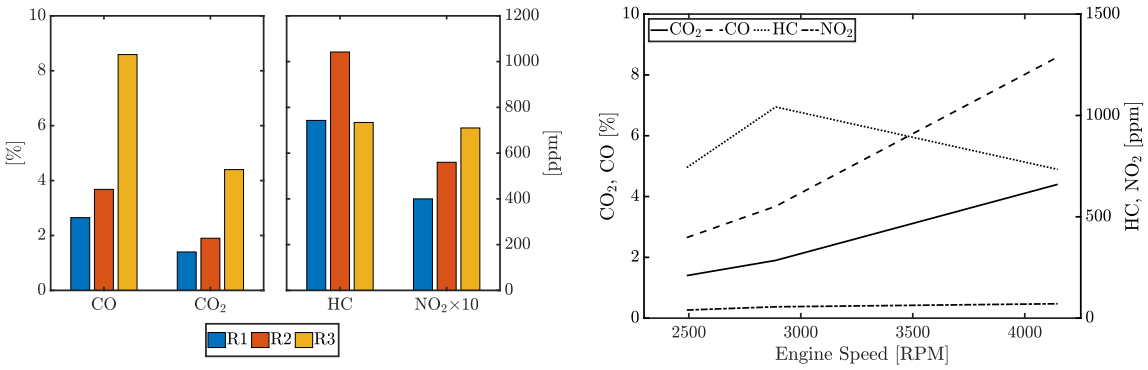


(a) Bar graph (b) Line plot

Figure 4.24: Emissions vs. engine speed [% and ppm] for BR1. ST = 15° $b$TDC.

of BR1 compared to BR0. This can also be seen in Figure 4.25b where BR1 operates almost 400 g/kWhr less $CO_2$ than BR0. There is however on average 20 g/kWhr more HC emissions in the BR1 case due to decreased combustion efficiency, and 0.4∼0.8 g/kWhr more $NO_2$ emissions due to the fuel bonded nitrogen in ammonia.

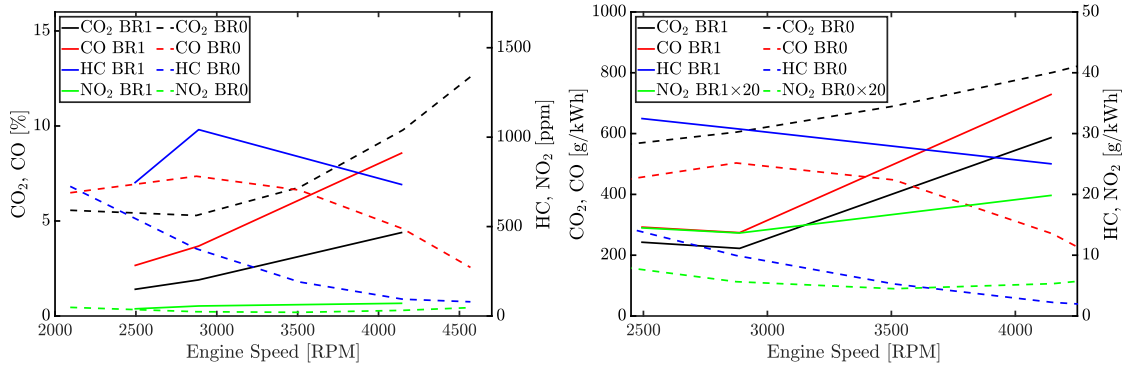


(a) [%] and [ppm] (b) [g/kWhr]

Figure 4.25: Emissions vs. engine speed for BR0 and BR1. ST = 10° $b$TDC for BR0 and ST = 15° $b$TDC for BR1.

### 4.3.3 Effects of Air Fuel Ratio (Lambda)

Figure 4.26 shows the gasoline and heptane emissions as a function of $\lambda$. As consistent with existing literature [47], both fuels follow the trends discussed in Section 4.3 for Figure 4.20. The $NO_2$ emissions for gasoline however continually decrease, rather than increase to a lean peak and then decrease. This abnormality is likely due to test variances or cycle-to-cycle variation.

Both fuels are compared in Figure 4.27, which exhibits similar behavior as dis-

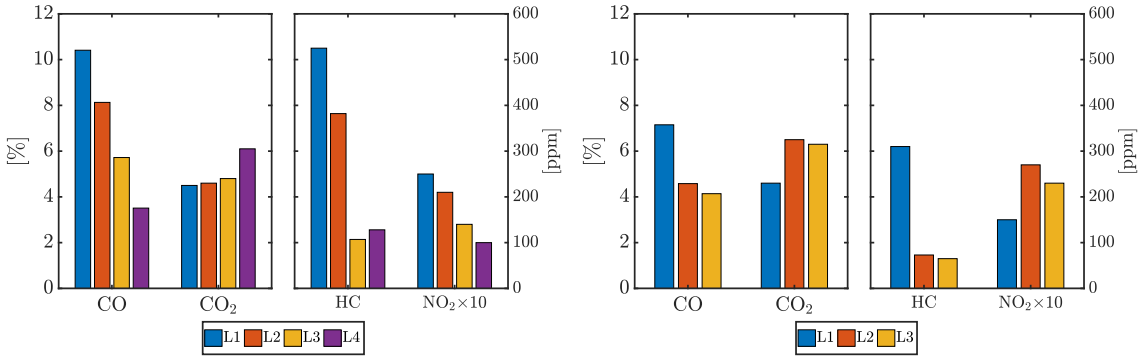


(a) Gasoline (b) Heptane

Figure 4.26: Emissions vs. lambda for 100% gasoline and 100% heptane. 3000 RPM, ST = 15° $b$TDC.

cussed before. In Figure 4.27b heptane exhibits slightly higher $NO_2$ than gasoline at lean conditions, due to a cycle-to-cycle variation. Generally the engine does not run hot enough to see significant thermal $NO_2$ increases. It is important to note from Figure 4.27b that heptane produces approximately 100 g/kWhr more $CO_2$ at lean conditions, and this increases to approximately 150 g/kWhr at rich conditions. This is because of the lower power output of heptane for the given spark angle.

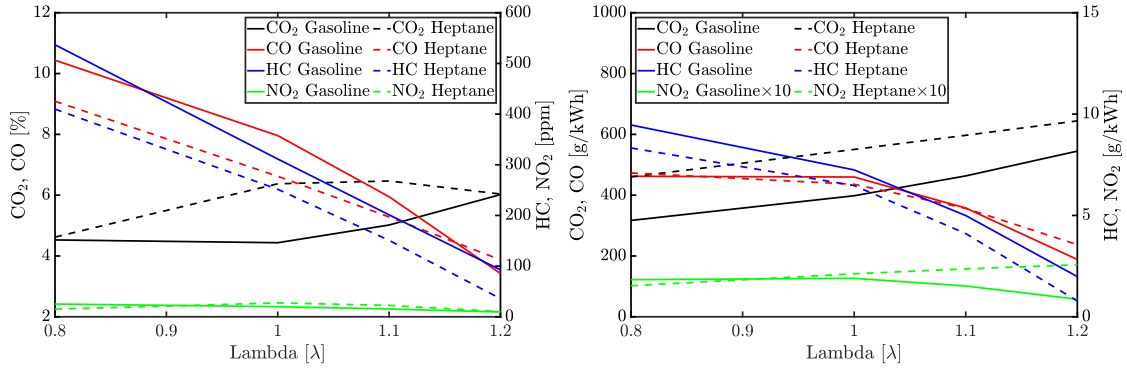


(a) Gasoline and heptane [% and ppm] (b) Gasoline and heptane [g/kWhr]

Figure 4.27: Emissions vs. lambda for 100% gasoline and 100% heptane. 3000 RPM, ST = 15° $b$TDC. 0.8 to 1 $\lambda$ for heptane is determined via polyfit.

### 4.3.4 Effects of Spark Timing

#### 4.3.4.1 Baseline Cases

Emissions as a function of spark timing is examined and discussed here. Figure 4.28 plots emissions of the baseline cases at different spark angles. It can be seen

that gasoline produces the least CO and $CO_2$ at case ST1 (-20° $b$TDC), suggesting favourable combustion and emission characteristics at higher spark timings. Both CO and $CO_2$ increase with reduced spark timing. This effect is attributed to the increased fuel consumption as seen in Figure 4.16a from Section 4.2.4.1.

Heptane on the other hand, shown in 4.28b, indicates that as spark advance is reduced, a more complete combustion process occurs. This is evident from Figure 4.16b in Section 4.2.4.1, which shows improved combustion efficiency with reduced spark advance for the same cases. As spark timing decreases the fuel and air appear to premix better, resulting in less CO and HC, and increased $CO_2$. $NO_2$ peaks at ST4 (-5° $b$TDC)) because at this spark timing less energy is being transferred into work and more into increased gas temperature.

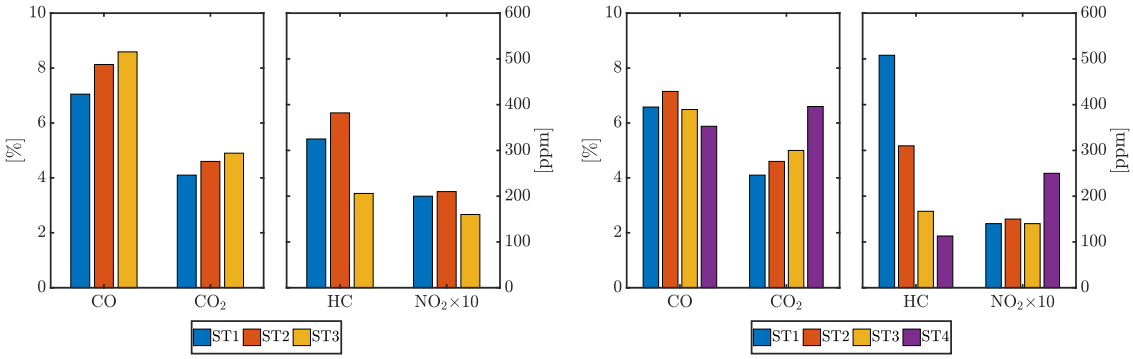


(a) Gasoline (b) Heptane

Figure 4.28: Emissions vs. spark timing for 100% gasoline and 100% heptane. $\lambda = 1$, 3000 RPM.

The gasoline and heptane emissions are compared in Figure 4.29, showing similar trends as previously discussed. It is interesting to see that heptane produces 60∼130 g/kWhr more $CO_2$ than gasoline on average.

#### 4.3.4.2 Blended Ammonia Cases

The emissions results with respect to spark timing for the BR0 and BR1 cases are presented here. Figure 4.30 shows the emissions for the BR1 case, which further suggests non-monotonic behaviour for spark timing. The lower HC emissions in the ST2 case are a result of non-dependence of spark timing and cycle-to-cycle variation.

It is worth noting that the BR1 case and BR0 case have consistent behaviour, as seen in Figure 4.31a. The HC emissions for BR1 are significantly higher than BR0, because of the decreased combustion efficiency. In Figure 4.31b it can be seen that

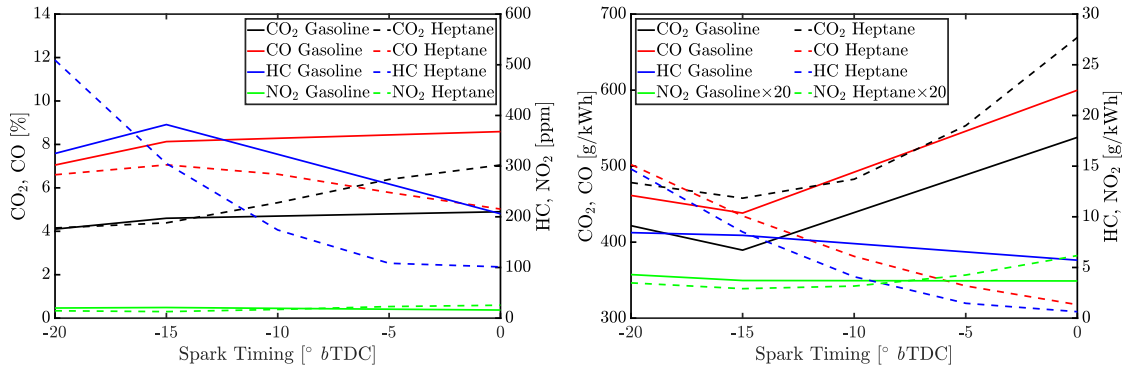


(a) [% and ppm] (b) [g/kWhr]

Figure 4.29: Emissions vs. spark timing for 100% gasoline and 100% heptane. $\lambda = 1$, 3000 RPM. -5 to 0° $b$TDC for heptane is determined via polyfit.

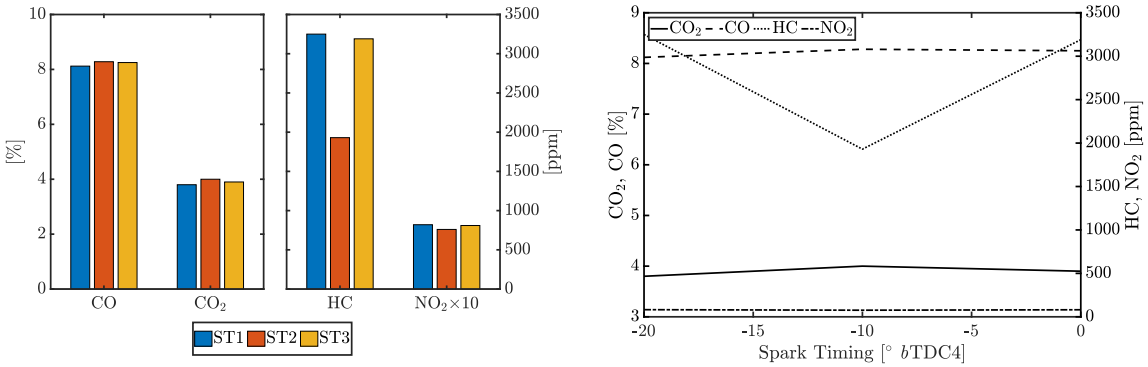


(a) Bar graph (b) Line plot

Figure 4.30: Emissions vs. spark timing [% and ppm] for BR1. 3000 RPM.

as spark timing is advanced all emissions for the BR0 and BR1 case trend downward. This is because of the increased power at advanced spark timing. It is evident that gasoline/ammonia blends produce the least emissions at high spark advance angles. Due to increased fuel mass in the BR1 case, $CO_2$ emissions are 100 g/kWhr worse at reduced spark angles, but dramatically improve to become 70 g/kWhr better at advanced angles. CO emissions are 400 g/kWhr worse at reduced spark timings for the BR1 case, but near identical to BR0 at a spark timing of -20°$b$TDC. The $NO_2$ is 1.5 g/kWhr higher for BR1 at reduced spark timings, and only 0.5 g/kWhr higher at advanced timings. An increase in $NO_2$ emissions can be expected because the fuel bonded nitrogen in ammonia. The HC emissions are 145 g/kWhr higher in the BR1 case to BR0 at reduced spark timings, but this difference declines to 67 g/kWhr at advanced spark angles. Reduced HC emissions at higher spark advance timings for the BR1 case are believed to be due to higher ammonia $\eta_c$.

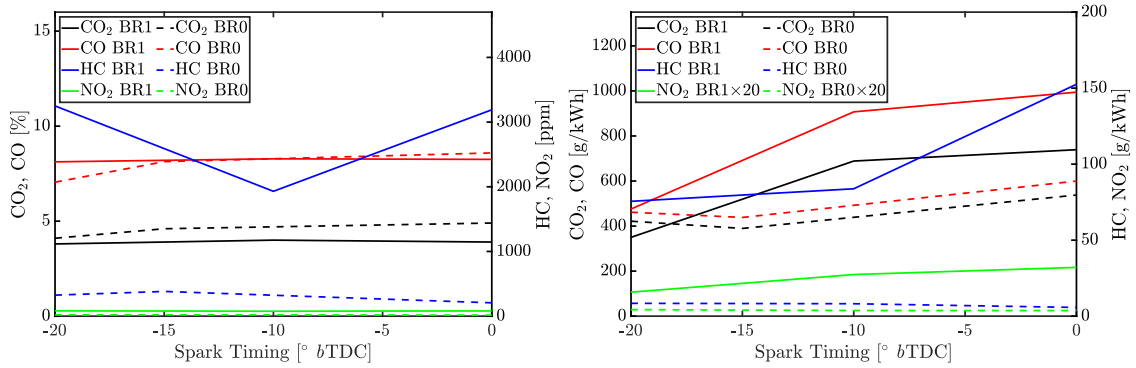


(a) [% and ppm]

(b) [g/kWhr]

Figure 4.31: Emissions vs. spark timing for BR0 and BR1. 3000 RPM.

### 4.3.5 *Section Summary*

The results presented in this section showed that the emissions of gasoline/ammonia blends have a strong correlation to spark advance timing because of increased combustion duration with ammonia content. The emissions of gasoline/ammonia blends are cleanest at high spark angles and can out perform baseline cases. The HC emissions for gasoline/ammonia blends are elevated in all cases due to poor combustion efficiency, however a reduction in these emissions are seen at higher engine speeds and spark angles. In the next chapter the main findings of this study are presented and recommendations for future studies are provided.

# Chapter 5

# Conclusions and Future Work

In this chapter the findings of this study are discussed and recommendations on future studies is provided. Section 5.1 examines the experimental results and draws conclusions. Section 5.2 provides recommendations on future work for continued research in ammonia blended fuels.

## 5.1 Conclusions

In this study an experimental investigation was conducted to examine the combustion and emission characteristics of ammonia blended fuels using a dual fuel spark-ignited internal combustion engine. Ammonia was explored as a clean alternative fuel, and gasoline and heptane were explored as combustion promoters for the ammonia. A parametric analysis was conducted using a single cylinder research engine that was modified to incorporate an electronic dual fuel injection system and a data acquisition system. In this study gaseous ammonia was port injected alongside the combustion promoter to allow for premixing. The study unfortunately was forced to reach completion early due to the COVID-19 pandemic, and heptane/ammonia blends were not tested.

The effects of engine speed, lambda, and spark advance timing were studied for baseline cases (100% gasoline and 100% heptane), and the effects of fuel blend ratio, engine speed, and spark timing were studied for gasoline/ammonia blends. Two fuel blends were tested, 70% $NH_3$ to 30% gasoline by mass and 80%-$NH_3$ to 20%-gasoline by mass. The main findings of these thesis were:

- When the 80% $NH_3$ to 20% gasoline case was tested, it was unable to reach a stable operation resulting in poor combustion and emissions characteristics.

Sufficient premixing was not achieved and the combustion of ammonia fuel was not promoted well by gasoline at this blend ratio. The 70% $NH_3$ to 30% gasoline case achieved a stable operation. It was evident from the combustion analysis that good premixing of the fuels and oxidizer took place as a result of the micro mixing characteristics of gaseous ammonia, which plays a pivotal role in sustaining combustion.

- Gasoline and heptane performed similarly in terms of power, torque, specific fuel consumption, and combustion efficiency. It has been found that heptane shows promising combustion characteristics at low spark advance timings due to a faster laminar flame speed, which is a desirable property for an ammonia combustion promoter. Gasoline performed best at mid range spark advance timings.

- The overall fuel consumption of the gasoline/ammonia blends were found to be significantly higher than baseline cases. This was due to an increased throttle position and fuel injection during these tests, as well as decreased energy content of the blended fuel.

- It has been found that the combustion efficiency of the engine decreased with the introduction of ammonia due either a sub-optimal fuel blend ratio or less than ideal premixing characteristics. The combustion efficiency of gasoline/ammonia blends improved with engine speed due to improved volumetric efficiency and premixing.

- The gasoline/ammonia blend produced a lower indicated power and torque, and higher specific fuel consumption than the baseline case at low spark timings. Peak power an torque were found to occur at lower engine speeds for gasoline/ammonia blends due to the lower flame speed of ammonia and the lower spark timing used. It has been found that as spark timing advanced, there was a significant improvement in power, torque, and specific fuel consumption. It is evident that gasoline/ammonia fuel blends require higher spark advancements to see the best results due to the low flame speed of ammonia.

- For emissions characteristics it has been found that ammonia content increased the amount of HC emissions measured in the exhaust due to decreased combustion efficiency. Increased engine speeds and spark advance have shown to reduce HC emissions.

- Gasoline/ammonia blends were found to be effective at decreasing carbon emissions when high spark advance timings were utilized. The is an effect of the slower flame speed of ammonia increasing combustion duration. When spark advance timings were -19° $b$TDC and higher at 3000 RPM, gasoline/ammonia blends produced less $CO_2$ and similar CO to the baseline cases. It is important to note that gasoline/ammonia blends were operated rich in these tests compared to stoichiometric gasoline. From presented data, it is presumed that stoichiometric gasoline/ammonia at maximum brake torque (MBT) timing could result in a further reduction in carbon emissions. $NO_2$ emissions increased slightly due to the fuel bonded nitrogen in ammonia.

From these findings it is evident that if gasoline/ammonia blends were tuned to MBT in a dual fuel SI engine, they could outperform baseline gasoline cases with respect to power, torque, and $CO_2$ emissions. Gasoline/ammonia cases showed promise and feasibility as a future alternative fuel with decreased carbon emissions and similar $NO_2$ emissions when compared to baseline cases. While heptane/ammonia tests were not conducted, heptane also shows promise as a potential combustion promoter with similar performance to gasoline, and a higher flame speed which is advantageous for ammonia. It is apparent that further testing is required to gain a better understanding of the combustion and emission characteristics of these ammonia fuel blends.

## 5.2 Future Work

Regarding ammonia fuels in internal combustion engines, there is still necessary research and development required before it could be effectively implemented into vehicles as a clean fuel. Further studies must be conducted comparing the different systems and combustion promoters, as well as a detailed economic analysis of ammonia dual fuel vehicles. Control strategies for dual fuel ammonia systems would also need to be developed to determine the optimal fuel blend ratios, air fuel ratios (lambda), and spark timing for a given driving conditions. Ammonia specific exhaust after treatment options would need to be developed to prevent any ammonia slip to the environment, and to reduce elevated $NO_x$ emissions.

It is recommended that combustion promoters such as E85 (85% ethanol and 15% gasoline) and hydrogen are explored due to their fast flame speeds and clean emissions. Forced induction applications and high compression ratios engines are also recommended to improve efficiency and take advantage of the high octane rating of ammonia. The high octane value and autoignition temperature of ammonia makes it

able to withstand high pressures and temperatures to allow for knock free combustion.

With respect to this present study, further testing is required to develop trends and gain a clearer understanding of the combustion and emission characteristics, especially for heptane/ammonia blends. A guideline for how these tests should be conducted has been provided in Appendixes A to D. If the current experimental unit were to be used for further research, ammonia slip monitoring should be implemented to measure ammonia combustion efficiency, and the issues discussed in Section 3.3 should be addressed.

# References


[1] W. W. Pulkrabek, *Engineering Fundamentals of the Internal Combustion Engine, 2nd Ed.* Upper Saddle River, NJ: Pearson Education, 2nd ed. 2004 ed., 2004.

[2] E. Bush, *Canada's Changing Climate Report.* Report, Environment Canada, 2019-04-01.

[3] E. A. Brohi, "Ammonia as fuel for internal combustion engines?," 2014.

[4] A. Yapicioglu and I. Dincer, "A review on clean ammonia as a potential fuel for power generators," *Renewable and Sustainable Energy Reviews*, vol. 103, pp. 96,108, 2019-04.

[5] A. J. Reiter and S.-C. Kong, "Combustion and emissions characteristics of compression-ignition engine using dual ammonia-diesel fuel," *Fuel*, vol. 90, no. 1, pp. 87,97, 2011.

[6] S. R. Turns, *An Introduction to Combustion: Concepts and Applications, 3rd Ed.* New York: McGraw-Hil, 3rd ed. 2012 ed., 2012.

[7] A. Valera-Medina, H. Xiao, M. Owen-Jones, W. David, and P. Bowen, "Ammonia for power," *Progress in Energy and Combustion Science*, vol. 69, pp. 63,102, 2018-11.

[8] C. Zamfirescu and I. Dincer, "Using ammonia as a sustainable fuel," *Journal of Power Sources*, vol. 185, no. 1, pp. 459,465, 2008.

[9] P. Dimitriou and R. Javaid, "A review of ammonia as a compression ignition engine fuel," *International Journal of Hydrogen Energy*, vol. 45, no. 11, pp. 7098 – 7118, 2020.

[10] J. B. Heywood, *Internal combustion engine fundamentals*. McGraw-Hill series in mechanical engineering, New York ;: McGraw-Hill, 1988.

[11] T. Anh, V. Duy, H. Thi, and H. Xa, "Experimental investigation on establishing the hcci process fueled by n-heptane in a direct injection diesel engine at different compression ratios," *Sustainability (Switzerland)*, vol. 10, no. 11, 2018.

[12] M. Balki, C. Sayin, and M. Canakci, "The effect of different alcohol fuels on the performance, emission and combustion characteristics of a gasoline engine," *Fuel*, vol. 115, no. C, pp. 901–906, 2012-10-11.

[13] S. McAllister, *Fundamentals of Combustion Processes*. Mechanical Engineering Series, New York, NY: Springer New York, 1st ed. 2011. ed., 2011.

[14] H. Kobayashi, A. Hayakawa, K. k. a. Somarathne, and E. c. Okafor, "Science and technology of ammonia combustion," *Proceedings of the Combustion Institute*, vol. 37, no. 1, pp. 109,133, 2019.

[15] F. Verkamp, M. Hardin, and J. Williams, "Ammonia combustion properties and performance in gas-turbine burners," *Symposium (International) on Combustion*, vol. 11, no. 1, pp. 985–992, 1967.

[16] C. Morch, A. Bjerre, M. Gottrup, S. Sorenson, and J. Schramm, "Ammonia/hydrogen mixtures in an si-engine: Engine performance and analysis of a proposed fuel system," *Fuel*, vol. 90, no. 2, pp. 854,864, 2011-02.

[17] J. Li, H. Huang, N. Kobayashi, Z. He, and Y. Nagai, "Study on using hydrogen and ammonia as fuels: Combustion characteristics and no x formation," *International Journal of Energy Research*, vol. 38, no. 9, pp. 1214,1223, 2014-07.

[18] M. G. Zabetakis, "Flammability characteristics of combustible gases and vapors.," *Bureau of Mines*, vol. Bulletin 627, p. 21, 1965.

[19] E. L. Belmont and J. L. Ellzey, "Lean heptane and propane combustion in a non-catalytic parallel-plate counter-flow reactor," *Combustion and Flame*, vol. 161, no. 4, pp. 1055 – 1062, 2014.

[20] M. Ciniviz and H. Köse, "Hydrogen use in internal combustion engine: A review," 04 2020.

[21] H. Takashi and T. Kimitoshi, "Laminar flame speeds of ethanol, n-heptane, iso octane air mixtures," 01 2006.

[22] Y. Li, M. Bi, B. Li, and W. Gao, "Explosion behaviors of ammonia–air mixtures," *Combustion Science and Technology*, vol. 190, no. 10, pp. 1804–1816, 2018.

[23] C. R. Ferguson and A. T. Kirkpatrick, *Internal Combustion Engines: Applied Thermosciences, 3rd Ed.* West Sussex, UK: John Wiley and Sons, 3rd ed. 2016 ed., 2016.

[24] D. P. Nolan, "14 - control of ignition sources," in *Handbook of Fire and Explosion Protection Engineering Principles* (D. P. Nolan, ed.), pp. 145 – 155, Oxford: William Andrew Publishing, 2011.

[25] M. Pochet, V. Dias, B. Moreau, F. Foucher, H. Jeanmart, and F. Contino, "Experimental and numerical study, under ltc conditions, of ammonia ignition delay with and without hydrogen addition," *Proceedings of the Combustion Institute*, vol. 37, no. 1, pp. 621 – 629, 2019.

[26] Q. Liu, X. Chen, J. Huang, Y. Shen, Y. Zhang, and Z. Liu, "The characteristics of flame propagation in ammonia/oxygen mixtures," *Journal of Hazardous Materials*, vol. 363, pp. 187 – 196, 2019.

[27] B. Shu, S. Vallabhuni, X. He, G. Issayev, K. Moshammer, A. Farooq, and R. Fernandes, "A shock tube and modeling study on the autoignition properties of ammonia at intermediate temperatures," *Proceedings of the Combustion Institute*, vol. 37, no. 1, pp. 205–211, 2019.

[28] A. Hayakawa, Y. Arakawa, R. Mimoto, K. K. A. Somarathne, T. Kudo, and H. Kobayashi, "Experimental investigation of stabilization and emission characteristics of ammonia/air premixed flames in a swirl combustor," *International Journal of Hydrogen Energy*, vol. 42, no. 19, pp. 14010–14018, 2017.

[29] A. Yapicioglu and I. Dincer, "Performance assesment of hydrogen and ammonia combustion with various fuels for power generators," *International Journal of Hydrogen Energy*, vol. 43, no. 45, pp. 21037–21048, 2018.

[30] L. Yu, W. Zhou, Y. Feng, W. Wang, J. Zhu, Y. Qian, and X. Lu, "The effect of ammonia addition on the low-temperature autoignition of n-heptane: An experimental and modeling study," *Combustion and Flame*, vol. 217, pp. 4 – 11, 2020.

[31] E. C. Okafor, Y. Naito, S. Colson, A. Ichikawa, T. Kudo, A. Hayakawa, and H. Kobayashi, "Experimental and numerical study of the laminar burning velocity

of ch4–nh3–air premixed flames," *Combustion and Flame*, vol. 187, pp. 185 – 198, 2018.

[32] P. F. HENSHAW, T. D'ANDREA, K. R. C. MANN, and D. S.-K. TING, "Premixed ammonia-methane-air combustion," *Combustion Science and Technology*, vol. 177, no. 11, pp. 2151–2170, 2005.

[33] J. W. Ku, S. Choi, H. K. Kim, S. Lee, and O. C. Kwon, "Extinction limits and structure of counterflow nonpremixed methane-ammonia/air flames," *Energy*, vol. 165, pp. 314 – 325, 2018.

[34] A. Valera-Medina, R. Marsh, J. Runyon, D. Pugh, P. Beasley, T. Hughes, and P. Bowen, "Ammonia–methane combustion in tangential swirl burners for gas turbine power generation," *Applied Energy*, vol. 185, pp. 1362 – 1371, 2017. Clean, Efficient and Affordable Energy for a Sustainable Future.

[35] M. Ezzat and I. Dincer, "Development and assessment of a new hybrid vehicle with ammonia and hydrogen," *Applied Energy*, vol. 219, pp. 226 – 239, 2018.

[36] J. Li, H. Huang, L. Deng, Z. He, Y. Osaka, and N. Kobayashi, "Effect of hydrogen addition on combustion and heat release characteristics of ammonia flame," *Energy*, vol. 175, pp. 604 – 617, 2019.

[37] A. Reiter and S.-C. Kong, "Demonstration of compression-ignition engine combustion using ammonia in reducing greenhouse gas emissions," *Energy and Fuels*, vol. 22, no. 5, pp. 2963–2971, 2008.

[38] J. Lasocki, M. Bednarski, and M. Sikora, "Simulation of ammonia combustion in dual-fuel compression-ignition engine," *IOP Conference Series: Earth and Environmental Science*, vol. 214, p. 012081, jan 2019.

[39] M. Pochet, I. Truedsson, F. Foucher, H. Jeanmart, and F. Contino, "Ammonia-hydrogen blends in homogeneous-charge compression-ignition engine," *SAE Technical Papers*, vol. 2017-24-0087, 09 2017.

[40] C. Gross, "Combustion and emissions characteristics of a compression-ignition engine using ammonia-dme mixtures," 2012.

[41] C. Lhuillier, P. Brequigny, F. Contino, and C. Mounaïm-Rousselle, "Experimental study on ammonia/hydrogen/air combustion in spark ignition engine conditions," *Fuel*, vol. 269, p. 117448, 2020.

[42] S. Grannell, "The operating features of a stoichiometric, ammonia and gasoline dual fueled spark ignition engine," 2008.

[43] S. O. Haputhanthri, T. T. Maxwell, J. Fleming, and C. Austin, "Ammonia and Gasoline Fuel Blends for Spark Ignited Internal Combustion Engines," *Journal of Energy Resources Technology*, vol. 137, 11 2015. 062201.

[44] K. Ryu, G. E. Zacharakis-Jutz, and S.-C. Kong, "Effects of gaseous ammonia direct injection on performance characteristics of a spark-ignition engine," *Applied Energy*, vol. 116, pp. 206 – 215, 2014.

[45] S. Frigo and R. Gentili, "Analysis of the behaviour of a 4-stroke si engine fuelled with ammonia and hydrogen," *International Journal of Hydrogen Energy*, vol. 38, no. 3, pp. 1607 – 1615, 2013. 2011 Zing International Hydrogen and Fuel Cells Conference: from Nanomaterials to Demonstrators.

[46] F. R. Westlye, A. Ivarsson, and J. Schramm, "Experimental investigation of nitrogen based emissions from an ammonia fueled si-engine," *Fuel*, vol. 111, pp. 239 – 247, 2013.

[47] R. M. R. Forum, "Pfc tuning and ca emissions," 2010.

# Appendix

## Appendix A: Future Gasoline Baseline Tests

Table A.1: Future gasoline baseline tests

| Gasoline | | | |
|---|---|---|---|
| Case ID | Engine Speed (RPM) | Lambda ($\lambda$) | Spark Advance ($^{\circ}b$TDC) |
| G_R1 | 2000 | 1 | MBT |
| G_R2 | 2500 | | |
| G_R3 | 3000 | | |
| G_R4 | 3500 | | |
| G_R5 | 4000 | | |
| G_R6 | 4500 | | |
| G_R7 | 5000 | | |
| G_L1 | 3000 | 0.8 | MBT |
| G_L2 | | 0.9 | |
| G_L3 | | 1 | |
| G_L4 | | 1.1 | |
| G_L5 | | 1.2 | |
| G_ST1 | 3000 | 1 | 25 |
| G_ST2 | | | 20 |
| G_ST3 | | | 15 |
| G_ST4 | | | 10 |
| G_ST5 | | | 5 |

# Appendix B: Future Heptane Baseline Tests

Table A.2: Future heptane baseline tests

| Heptane | | | |
|---|---|---|---|
| Case ID | Engine Speed (RPM) | Lambda ($\lambda$) | Spark Advance ($^{\circ}b$TDC) |
| H_R1 | 2000 | 1 | MBT |
| H_R2 | 2500 | | |
| H_R3 | 3000 | | |
| H_R4 | 3500 | | |
| H_R5 | 4000 | | |
| H_R6 | 4500 | | |
| H_R7 | 5000 | | |
| H_L1 | 3000 | 0.8 | MBT |
| H_L2 | | 0.9 | |
| H_L3 | | 1 | |
| H_L4 | | 1.1 | |
| H_L5 | | 1.2 | |
| H_ST1 | 3000 | 1 | 25 |
| H_ST2 | | | 20 |
| H_ST3 | | | 15 |
| H_ST4 | | | 10 |
| H_ST5 | | | 5 |

# Appendix C: Future Gasoline/Ammonia Tests

Table A.3: Future gasoline/ammonia tests

Gasoline – Ammonia

| Case ID | Blend Ratio ($NH_3$-Gasoline) | Engine Speed (RPM) | Lambda ($\lambda$) | Spark Advance ($^\circ b$TDC) |
|---|---|---|---|---|
| GA_BR1 | 20-80 | 3000 | 1 | MBT |
| GA_BR2 | 30-70 | | | |
| GA_BR3 | 40-60 | | | |
| GA_BR4 | 50-50 | | | |
| GA_BR5 | 60-40 | | | |
| GA_BR6 | 70-30 | | | |
| GA_BR7 | 80-20 | | | |
| GA_R1 | Each Ratio | 2000 | 1 | MBT |
| GA_R2 | | 2500 | | |
| GA_R3 | | 3000 | | |
| GA_R4 | | 3500 | | |
| GA_R5 | | 4000 | | |
| GA_R6 | | 4500 | | |
| GA_R7 | | 5000 | | |
| GA_L1 | Each Ratio | 3000 | 0.8 | MBT |
| GA_L2 | | | 0.9 | |
| GA_L3 | | | 1 | |
| GA_L4 | | | 1.1 | |
| GA_L5 | | | 1.2 | |
| GA_ST1 | Each Ratio | 3000 | 1 | 25 |
| GA_ST2 | | | | 20 |
| GA_ST3 | | | | 15 |
| GA_ST4 | | | | 10 |
| GA_ST5 | | | | 5 |

# Appendix D: Planned Heptane/Ammonia Tests

Table A.4: Future heptane/ammonia tests

Heptane – Ammonia

| Case ID | Blend Ratio ($NH_3$-Heptane) | Engine Speed (RPM) | Lambda ($\lambda$) | Spark Advance ($^\circ b$TDC) |
|---|---|---|---|---|
| HA_BR1 | 20-80 | 3000 | 1 | MBT |
| HA_BR2 | 30-70 | | | |
| HA_BR3 | 40-60 | | | |
| HA_BR4 | 50-50 | | | |
| HA_BR5 | 60-40 | | | |
| HA_BR6 | 70-30 | | | |
| HA_BR7 | 80-20 | | | |
| HA_R1 | Each Ratio | 2000 | 1 | MBT |
| HA_R2 | | 2500 | | |
| HA_R3 | | 3000 | | |
| HA_R4 | | 3500 | | |
| HA_R5 | | 4000 | | |
| HA_R6 | | 4500 | | |
| HA_R7 | | 5000 | | |
| HA_L1 | Each Ratio | 3000 | 0.8 | MBT |
| HA_L2 | | | 0.9 | |
| HA_L3 | | | 1 | |
| HA_L4 | | | 1.1 | |
| HA_L5 | | | 1.2 | |
| HA_ST1 | Each Ratio | 3000 | 1 | 25 |
| HA_ST2 | | | | 20 |
| HA_ST3 | | | | 15 |
| HA_ST4 | | | | 10 |
| HA_ST5 | | | | 5 |